Anomalous Transverse Response in Non-collinear Antiferromagnets Mn_3X (X = Sn, Ge)

Zengwei Zhu

Wuhan National High Magnetic Field Center
and School of Physics
Huazhong University of Science and Technology

Where is Wuhan?

Collaborators

国家脉冲强磁场科学中心

ESPCI, FR

Weizmann Institute of Science, Israel

Ecole Polytechnique &College de France

Xiaokang Li,

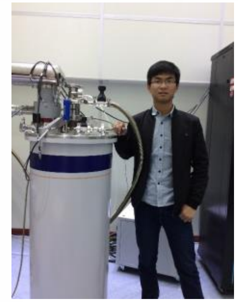

Liangcai Xu, Xiufang Lu, Linchao Ding Jinhua Wang Mingsong Shen

Kamran Behnia, Benoit Fauque, Clement Collignon

Binghai Yan, Huixia Fu

Alaska Subedi

University of California, Santa Barbara

Leon Balents

Outline

I. Short Introduction to Anomalous Hall Effect (AHE)

II. Discovery of AHE in Mn_3Sn and Mn_3Ge

III. Thermal and thermoelectric counterparts of the AHE and Wiedemann-Franz law in Mn_3Sn

IV. Finite-temperature violation of the anomalous transverse Wiedemann-Franz law in absence of inelastic scattering in Mn_3Ge

V. Momentum-space and real-space Berry curvatures in Mn_3Sn

VI. Chiral domain walls of Mn_3Sn and their memory

Anomalous Hall effect :

$$\rho_H = R_0 B + R_s \mu_0 M$$

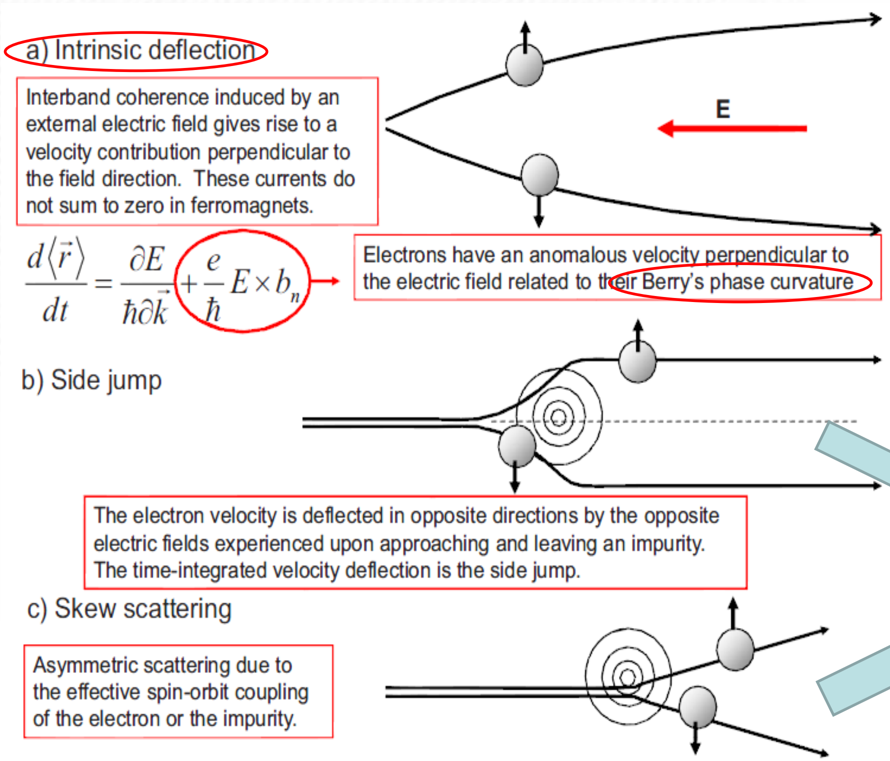

Intrinsic mechanism: depends on the band structure and is independent of scattering, related to Berry's phase curvature.

Extrinsic mechanism: related to scattering from spin-orbit coupling or impurity.

N. Nagaosa et al., Rev. Mod. Phys. 82, 1539 (2010)

Theoretical prediction:

PRL 112, 017205 (2014) PHYSICAL REVIEW LETTERS week ending 10 JANUARY 2014

Anomalous Hall Effect Arising from Noncollinear Antiferromagnetism

Hua Chen, Qian Niu, and A. H. MacDonald
Department of Physics, University of Texas at Austin, Austin, Texas 78712, USA
(Received 3 October 2013; published 10 January 2014)

As established in the very early work of Edwin Hall, ferromagnetic conductors have an anomalous Hall conductivity contribution that cannot be attributed to Lorentz forces and therefore survives in the absence of a magnetic field. These anomalous Hall conductivities are normally assumed to be proportional to magnetization. We use symmetry arguments and first-principles electronic structure calculations to counter this assumption and to predict that Mn_3Ir, a high-temperature antiferromagnet that is commonly employed in spin-valve devices, has a large anomalous Hall conductivity.

Theoretical prediction: a non-collinear antiferromagnet will show a large AHE with no magnetization!

EPL, 108 (2014) 67001 www.epljourna
doi: 10.1209/0295-5075/108/67001

Non-collinear antiferromagnets and the anomalous Hall effect

J. Kübler[1] and C. Felser[2]

[1] *Institut für Festkörperphysik, Technische Universität Darmstadt - D-64289 Darmstadt, Germany*
[2] *Max Planck Institute for Chemical Physics of Solids - D-01187 Dresden, Germany*

received 10 November 2014; accepted 2 December 2014
published online 10 December 2014

PACS 73.43.Cd – Theory and modeling
PACS 75.50.Ee – Antiferromagnetics
PACS 75.70.Tj – Spin-orbit effects

Abstract – The anomalous Hall effect is investigated theoretically by employing density functional calculations for the non-collinear antiferromagnetic order of the hexagonal compounds Mn_3Ge and Mn_3Sn using various planar triangular magnetic configurations as well as unexpected non-planar configurations. The former give rise to anomalous Hall conductivities (AHC) that are found to be extremely anisotropic. For the planar cases the AHC is connected with Weyl points in the energy-band structure. If this case were observable in Mn_3Ge, a large AHC of about $\sigma_{zx} \approx 900\,(\Omega\text{cm})^{-1}$ should be expected. However, in Mn_3Ge it is the non-planar configuration that is energetically favored, in which case it gives rise to an AHC of $\sigma_{xy} \approx 100\,(\Omega\text{cm})^{-1}$. The non-planar configuration allows a quantitative evaluation of the topological Hall effect that is seen to determine this value of σ_{xy} to a large extent. For Mn_3Sn it is the planar configurations that are predicted to be observable. In this case the AHC can be as large as $\sigma_{yz} \approx 250\,(\Omega\text{cm})^{-1}$.

The AHE calculation for the non-collinear antiferromagnetic Mn_3Ge and Mn_3Sn

Discovery of AHE in Mn_3Sn

LETTER

doi:10.1038/nature15723

Large anomalous Hall effect in a non-collinear antiferromagnet at room temperature

Satoru Nakatsuji[1,2], Naoki Kiyohara[1] & Tomoya Higo[1]

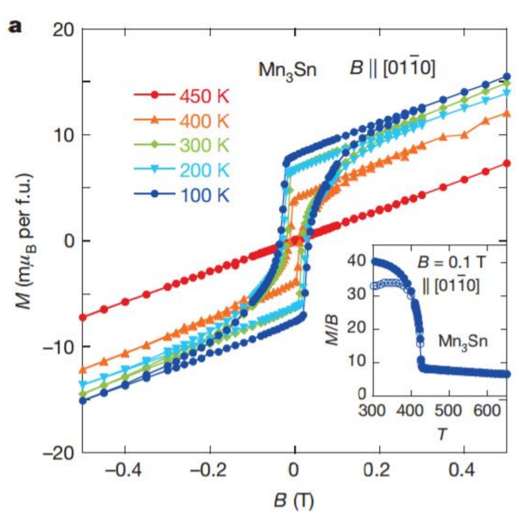

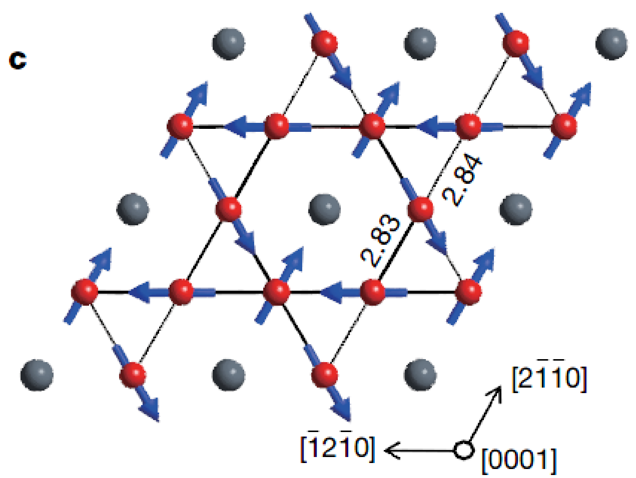

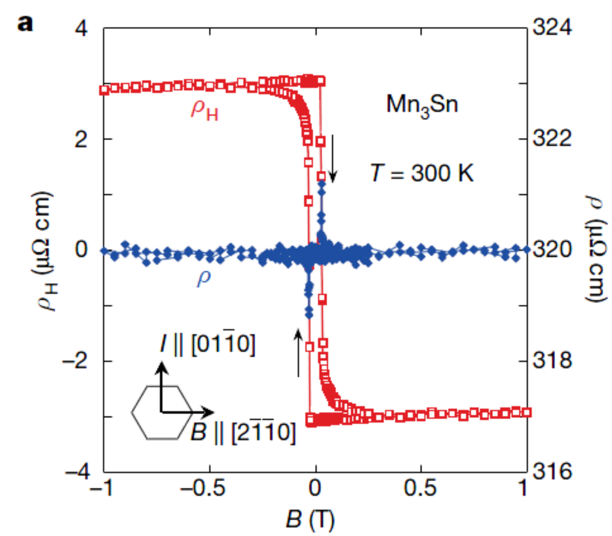

Discovery of AHE in Mn_3Sn

Journal of Magnetism and Magnetic Materials 70 (1987) 249–251 249
North-Holland, Amsterdam

SPIN STRUCTURE AND WEAK FERROMAGNETISM OF Mn_3Sn

H. OHMORI, S. TOMIYOSHI, H. YAMAUCHI and H. YAMAMOTO
The Research Institute for Iron, Steel and Other Metals, Tohoku University, Sendai, Japan

The compound Mn_3Sn shows an interesting magnetic behavior. A triangular screw spin structure has been observed below 250 K, whose period is independent of temperature. The screw structure is sensitive to heat treatment, alloy composition and impurity content.

The triangular spin order persists in a finite temperature window: 200 K< T< 420 K

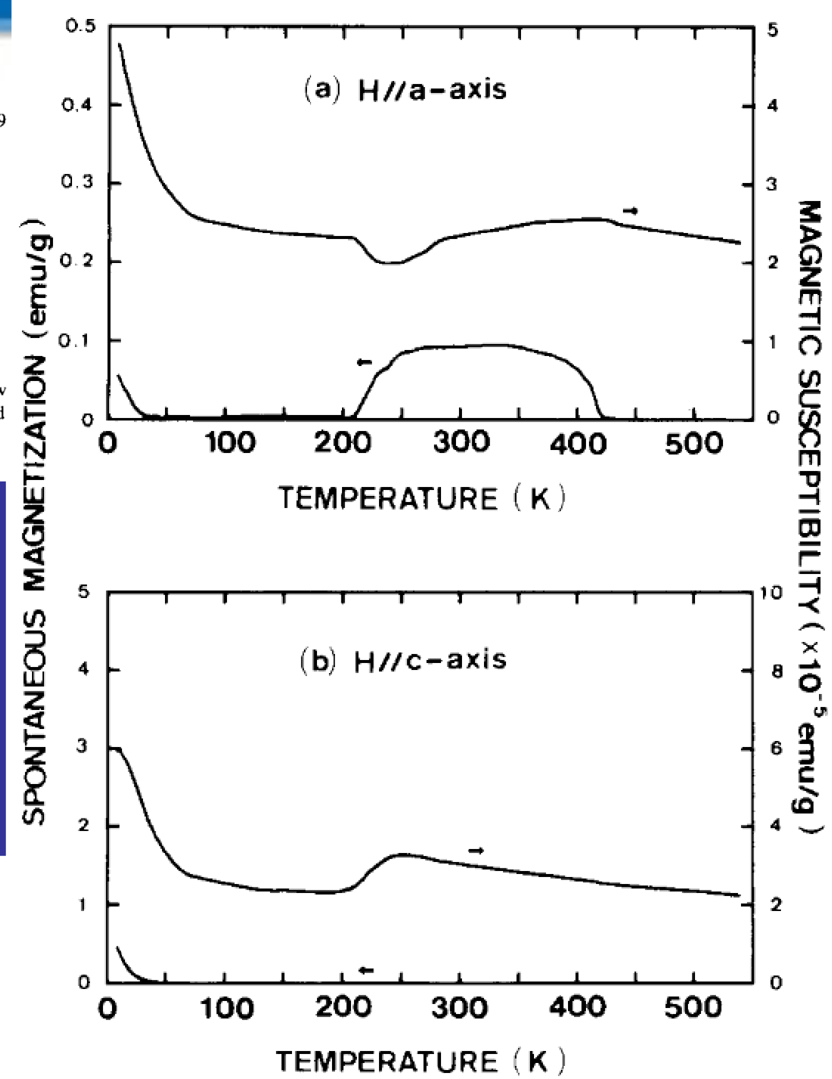

c

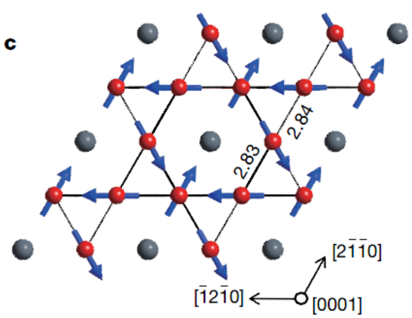

Flow of heat and charge

Kelvin relation, (1860) Onsager relation (1930)

$$\vec{J}_e = \sigma \vec{E} - \alpha \vec{\nabla} T$$

$$\vec{J}_Q = \beta \vec{E} - \kappa \vec{\nabla} T$$

$$\beta = \alpha T$$

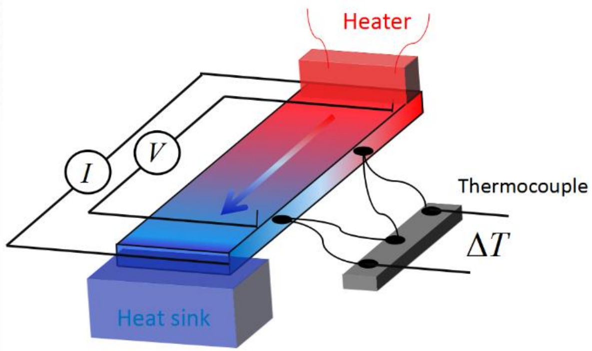

Four vectors

J_e : charge current density
J_Q : heat current density
E : electric field
∇T : thermal gradient

In general, σ(electric conductivity), α(thermo-electic conductivity) and κ(thermal conductivity) are tensors ! Off-diagonal components emerge in presence of magnetic field:

- **σ_{xy} Hall effect**
- **α_{xy} Nernst effect**
- **κ_{xy} Righi-Leduc effect**

Basic properties of Mn_3Sn:

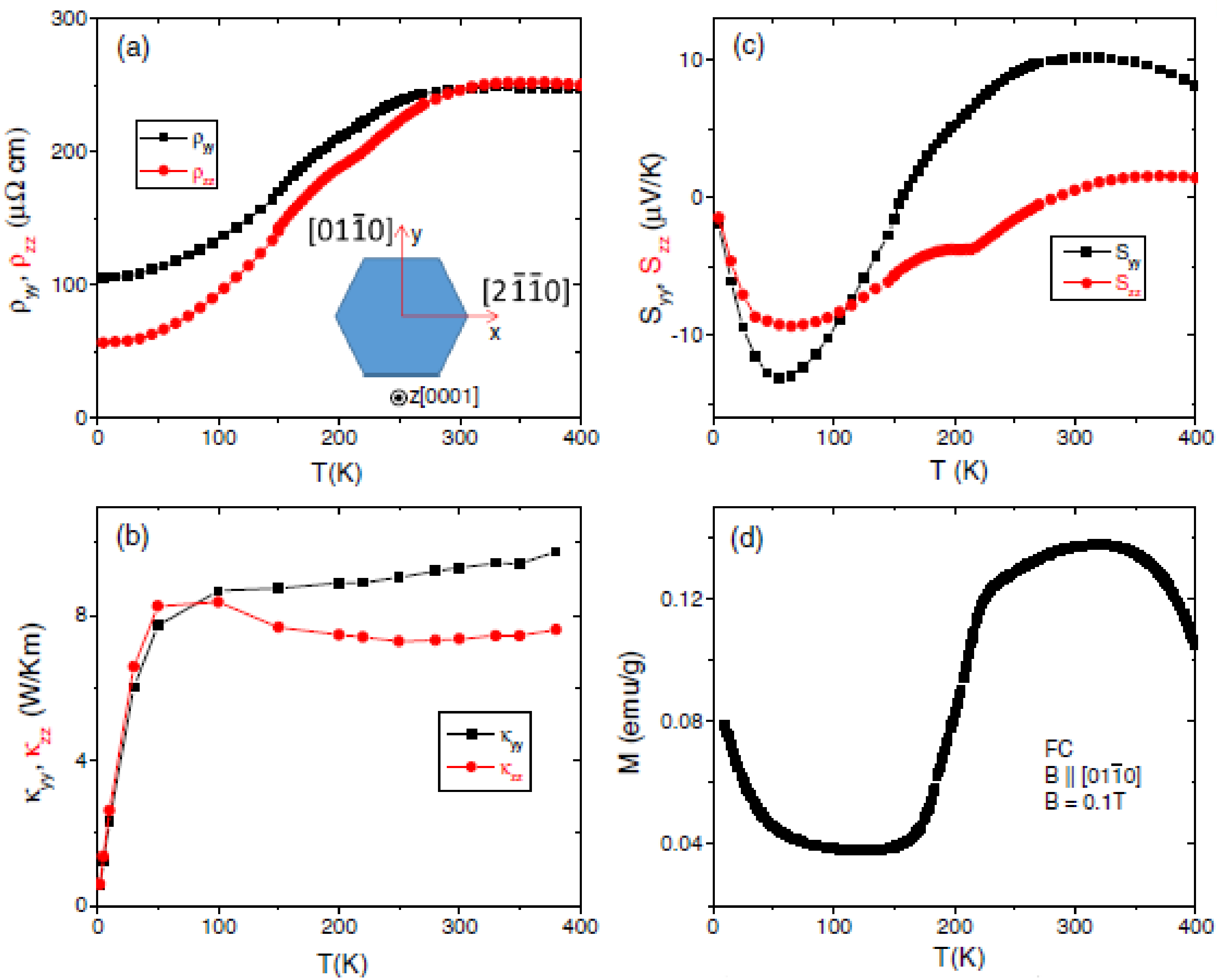

The triangular spin order 200 - 425 K

Thermal and thermoelectric counterparts of the AHE

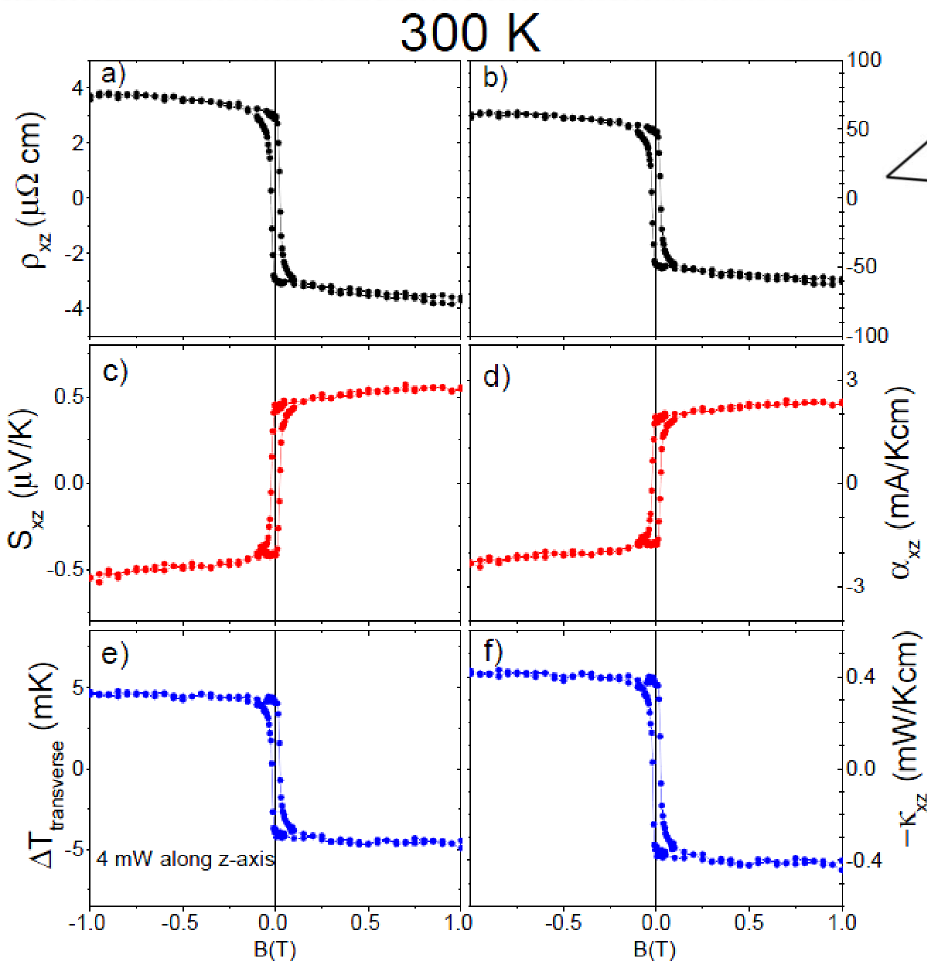

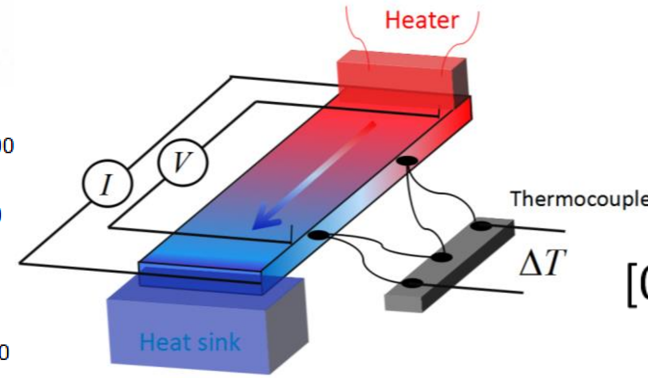

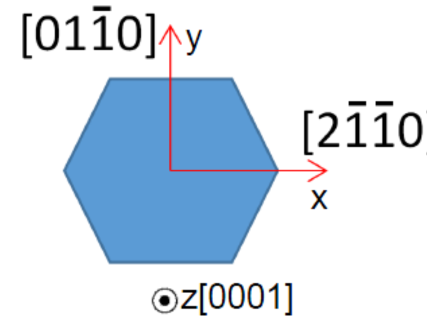

Easily detectable transverse responses: Anomalous Hall, Nernst and Righi-Leduc Effects in Mn_3Sn!

Xiaokang Li, et al., Z.Z*, K.B* PRL 119, 056601 (2017)

VOLUME 93, NUMBER 20 PHYSICAL REVIEW LETTERS week ending 12 NOVEMBER 2004

Berry Curvature on the Fermi Surface: Anomalous Hall Effect as a Topological Fermi-Liquid Property

F. D. M. Haldane

Department of Physics, Princeton University, Princeton New Jersey 08544-0708, USA

(Received 28 June 2004; revised manuscript received 20 October 2004; published 11 November 2004)

The intrinsic anomalous Hall effect in metallic ferromagnets is shown to be controlled by Berry phases accumulated by adiabatic motion of quasiparticles on the Fermi surface, and is purely a Fermi-liquid property, not a bulk Fermi sea property like Landau diamagnetism, as has been previously supposed. Berry phases are a new topological ingredient that must be added to Landau Fermi-liquid theory in the presence of broken inversion or time-reversal symmetry.

DOI: 10.1103/PhysRevLett.93.206602 PACS numbers: 72.15.–v, 73.43.–f

$$\kappa_0^{ab}(\mu) = \frac{\pi^2}{3}\frac{k_B^2 T}{e^2}\sigma_0^{ab}(\mu), \qquad \alpha_0^{ab}(\mu) = e\frac{\partial \kappa_0^{ab}(\mu)}{\partial \mu}.$$

The Fermi-surface vs. Fermi sea debate

$$\sigma_{ij}^{A} = \frac{-e^2}{\hbar}\sum_n \int_{BZ} \frac{d^3k}{(2\pi)^3} f_n(k)\Omega_n^k(k)$$

Fermi sea

"..In particular, we show that the common belief that (the nonquantized part of) the intrinsic anomalous Hall conductivity of a ferromagnetic metal is entirely a Fermi-surface property, is incorrect."

Y. Chen, D. L. Bergman, and A. A. Burkov Phys. Rev. B 88, 125110 (2013)

$$\sigma_{ij}^{A} = \frac{-e^2}{\hbar}\sum_n \int_{S_n} \frac{d^2k}{(2\pi)^2} [\Omega_n^k(k).\hat{n}(k)]\mathbf{k}$$

Fermi-surface

"We point out that, contrary to an assertion by Chen et al. [Phys. Rev. B 88, 125110 (2013)], the nonquantized part of the intrinsic anomalous Hall conductivity can indeed be expressed as a Fermi-surface property even when Weyl points are present in the band structure."

David Vanderbilt, Ivo Souza, and F. D. M. Haldane, Phys. Rev. B 92, 1117101 (2014)

The case of iron

VOLUME 92, NUMBER 3 PHYSICAL REVIEW LETTERS week ending 23 JANUARY 2004

First Principles Calculation of Anomalous Hall Conductivity in Ferromagnetic bcc Fe

Yugui Yao,[1,2,3] Leonard Kleinman,[1] A. H. MacDonald,[1] Jairo Sinova,[4,1] T. Jungwirth,[5,1] Ding-sheng Wang,[3] Enge Wang,[2,3] and Qian Niu[1]

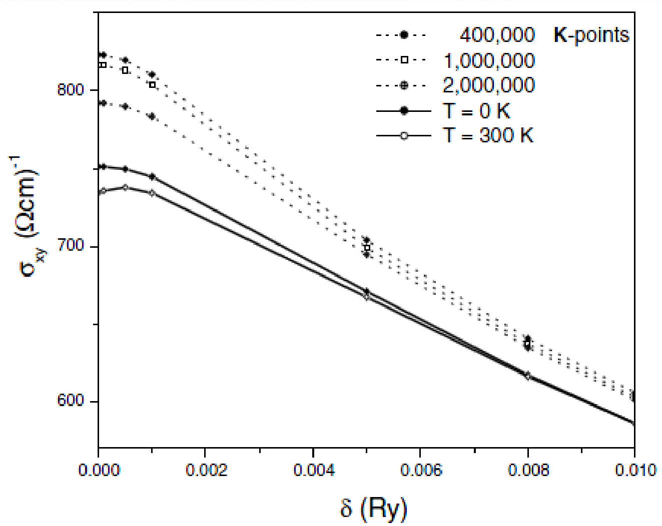

FIG. 1. Anomalous Hall effect vs δ with different numbers of $\mathbf{k}$ points in full Brillouin zone. Here δ is introduced by adding δ^2 to the denominator in Eq. (4). The dotted lines are obtained (for zero temperature) using a different number of $\mathbf{k}$ points. The solid lines are obtained by an adaptive mesh refinement method.

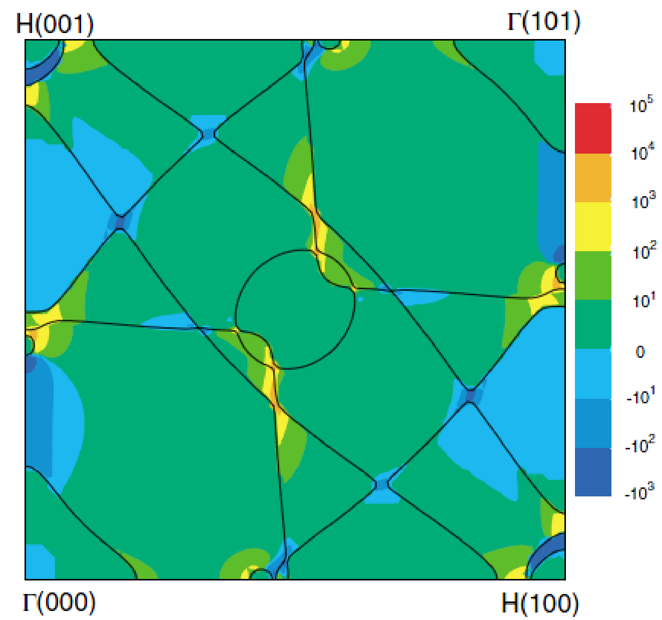

FIG. 3 (color). Fermi surface in (010) plane (solid lines) and Berry curvature $-\Omega^z(\mathbf{k})$ in atomic units (color map).

σ_{xy}^{A}**(Theory) ~750 Ωcm^{-1}**

PHYSICAL REVIEW B **92**, 085138 (2015)

Chiral degeneracies and Fermi-surface Chern numbers in bcc Fe

Daniel Gosálbez-Martínez,[1,2] Ivo Souza,[1,3] and David Vanderbilt[4]

[1] *Centro de Física de Materiales, Universidad del País Vasco, 20018 San Sebastián, Spain*

[2] *Donostia International Physics Center, 20018 San Sebastián, Spain*

[3] *Ikerbasque Foundation, 48013 Bilbao, Spain*

[4] *Department of Physics and Astronomy, Rutgers University, Piscataway, New Jersey 08854-8019, USA*

(Received 28 May 2015; published 21 August 2015)

The two picture of the AHE give the same number!

Fermi Sea

TABLE IV. Band-by-band decomposition of the AHC of bcc Fe. In the three middle columns the dimensionless AHC is further decomposed according to Eq. (50).

Band n	$\mathcal{K}^{(\Omega)}_{n3}$	$\mathcal{K}^{(\chi)}_{n3}$	$\mathcal{K}_{n3}$	AHC (S/cm)
1	2	0.51	2.51	−3394
2	−6	3.03	−2.97	4018
3	2	1.96	3.96	−5345
4	6	−8.85	−2.85	3840
5	−8.01	6.22	−1.79	2413
6	−7.80	3.27	−4.53	6111
7	14.12	−6.44	7.68	−10 368
8	−3.17	−0.31	−3.48	4702
9	−0.53	1.33	0.80	−1076
10	0.83	−0.72	0.11	−146
Total	−0.56	0	−0.56	755

Fermi Surface

TABLE V. Decomposition of the AHC of bcc Fe into nonquantized Fermi-sheet contributions. Symmetry-related sheets are grouped in the same row, and they contribute equal amounts. The two pockets $(10_6, 10_7)$ [group VII(b)] with opposite Chern numbers are treated as a single "composite sheet" and assigned a joint AHC contribution. The shortest distance from each Fermi sheet to a chiral PN on the same band is also indicated.

Band n	Sheet a	Group label	Distance to a PN $(2\pi/a)$	AHC (S/cm)	
5	1	IV	0.30	9	
6	1	III	0.02	−274	
7	1	V	0.06	459	
7	2,3,4,5	VIII(a)	0.01	−203	×4
7	6,7	VIII(b)	0.09	100	×2
8	1	II	0.03	242	
9	1	I	0.02	714	
10	1	VI	0.10	58	
10	2,3,4,5	VII(a)	0.31	−1	×4
10	6,7	VII(b)	0.01	167	
Total				759	

σ^{A}_{xy}(Theory) ~750 Scm^{-1}

How can thermal transport address this issue?

Semiclassic transport and Berry curvature

$$\dot{r} = \frac{1}{\hbar}\frac{\partial \epsilon_{n(\mathbf{k})}}{\partial \mathbf{k}} + \dot{\mathbf{k}} \times \Omega_n(\mathbf{k})$$

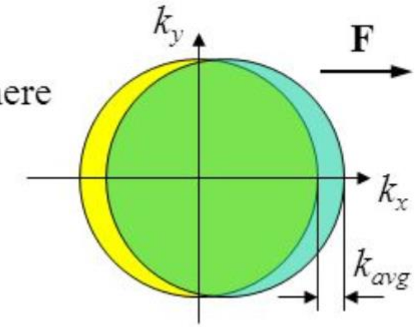

In presence of electric field: $\dot{k} = -eE/\hbar$ → **Anom. Hall**

In presence of a thermal gradient: $\dot{k} = -S_k \nabla T/\hbar$ → **Anom.Nernst &Righi-Leduc**

Only Fermi surface quasi-particles have an entropy, S_K !

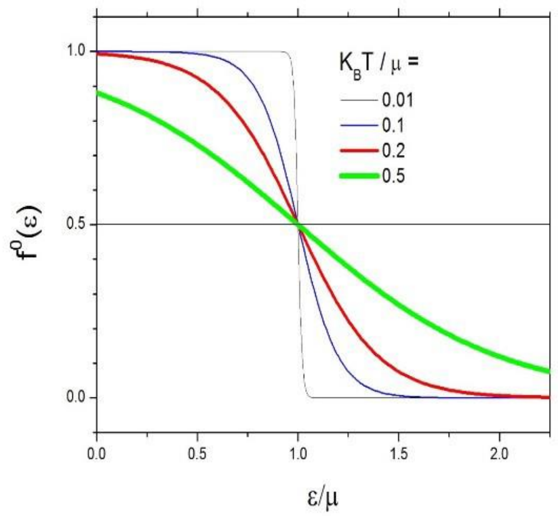

The Wiedemann-Franz law and the surface-sea debate!

$$L_{xy}^{A} = \frac{\kappa_{xy}^{A}}{T\sigma_{xy}^{A}} = \frac{\pi^2}{3}\left(\frac{k_B}{e}\right)^2$$

In the Fermi-sea picture, an accident!

In the Fermi-surface picture, indispensable!

Implications of the magnitude of the thermal and thermoelectric response in Mn_3Sn

The validation of WF law

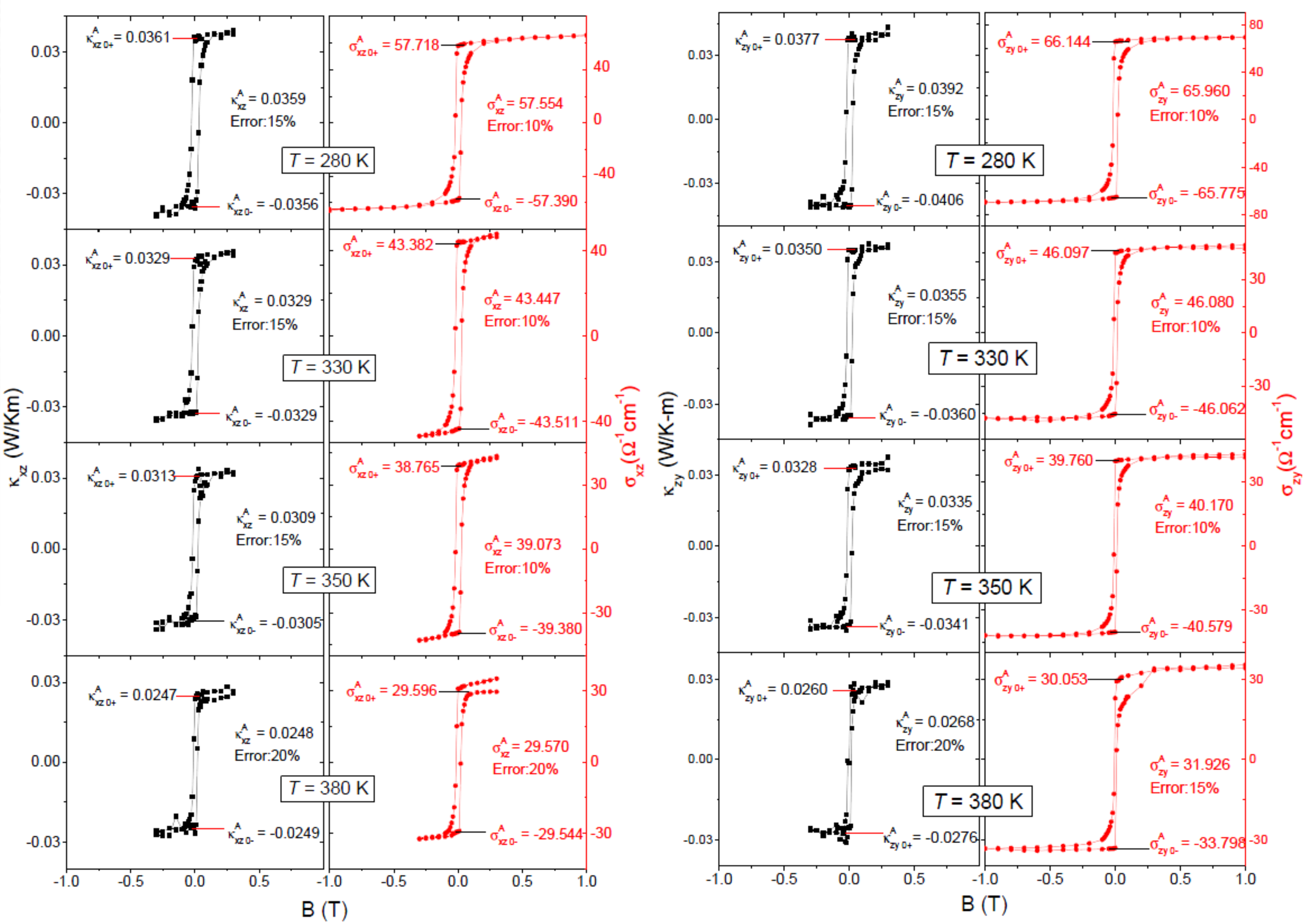

Robustness of the WF Law

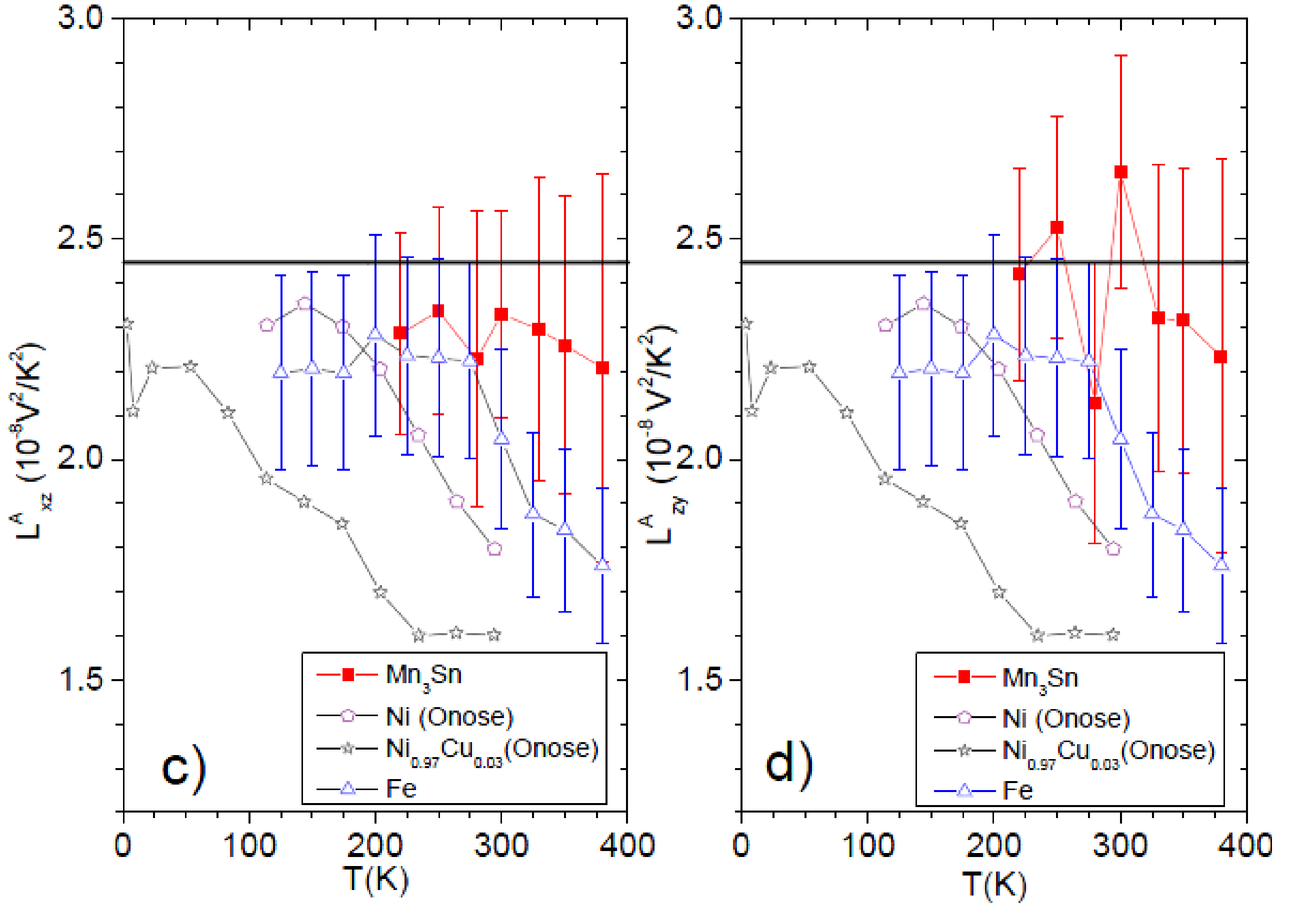

In Mn_3Sn, in contrast to common ferromagnets, there is no downward finite-temperature deviation from the Sommerfeld value.

No inelastic scattering contribution to Anomalous Hall response!

The inelastic scattering

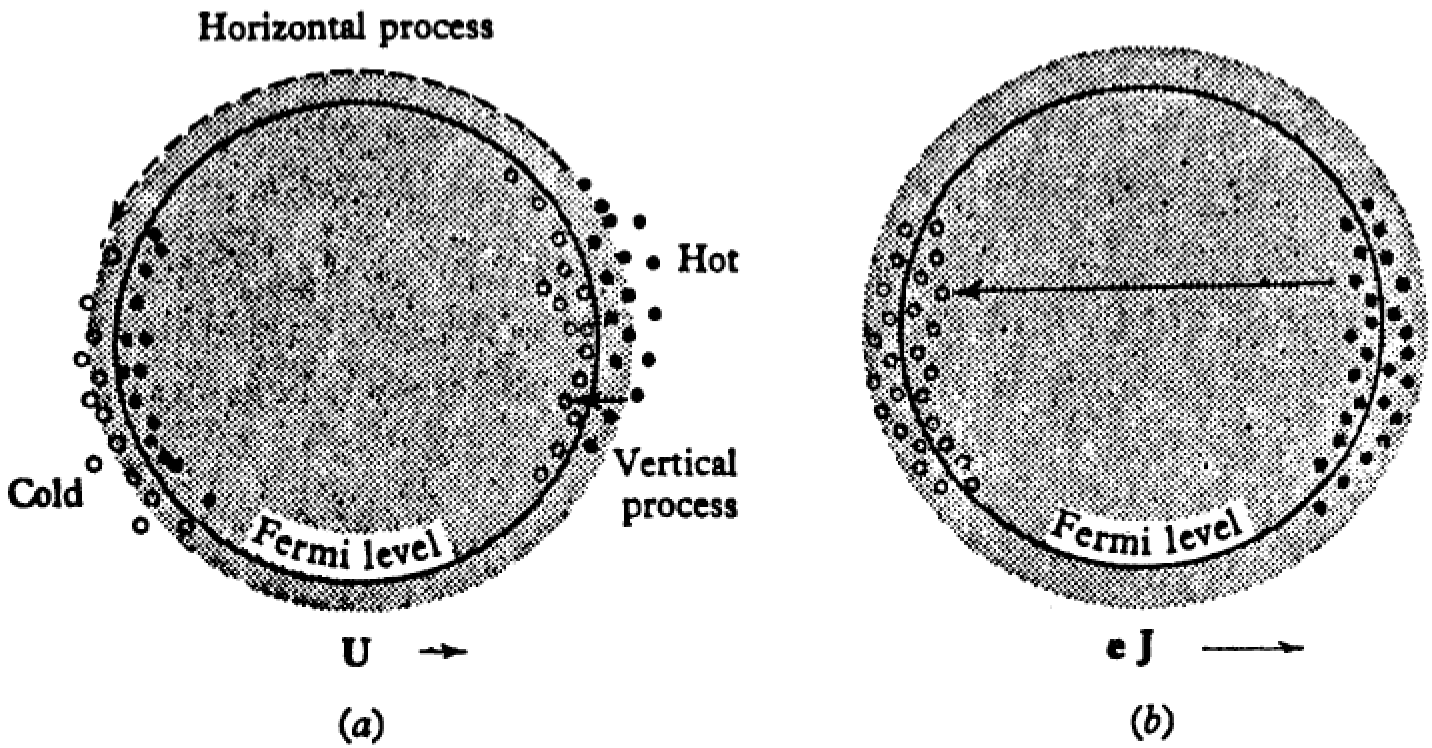

Fig. 127. Electron distributions, and scattering processes: (*a*) in thermal conduction; (*b*) in electrical conduction.

J. Ziman, Principles of the Theory of Solids, Cambridge University Press (1972).

The small-angle inelastic collisions decay the momentum flow less efficiently than the energy flow both for electron-phonon and electron-electron.

T-dependence of the magnetization

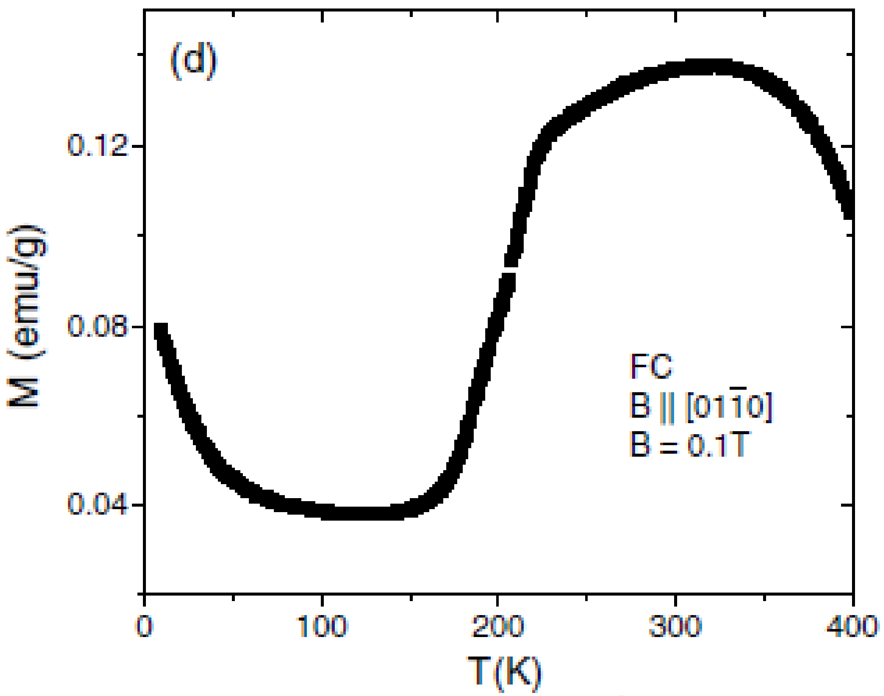

Mn_3Sn

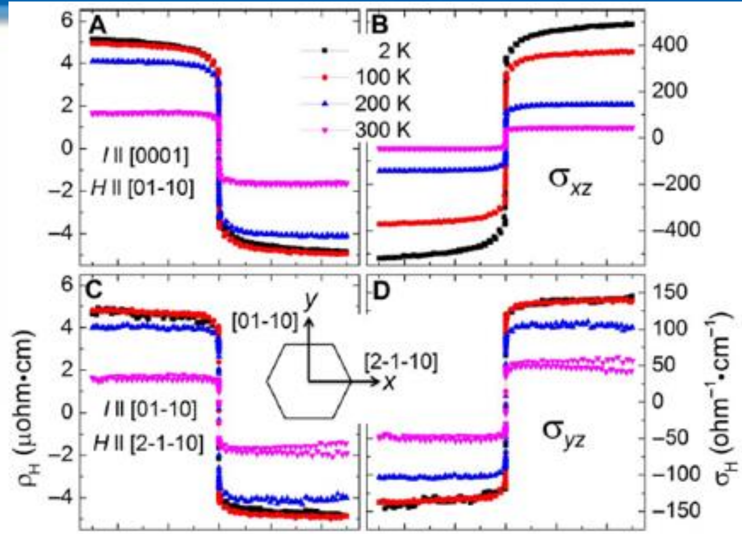

Nayak et al., Sci. Adv. 2, e1501870 (2016)

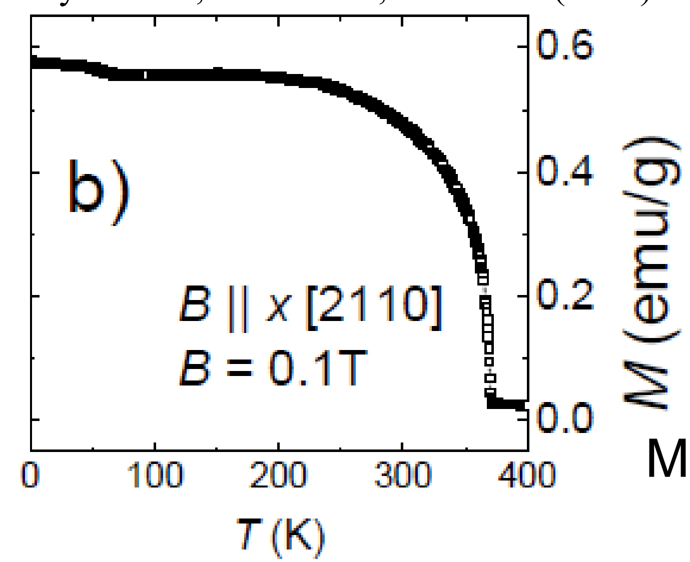

Mn_3Ge

In contrast to Mn_3Sn, in Mn_3Ge the triangular spin order persists down to T=0!

Anomalous transverse coefficients in Mn_3Ge

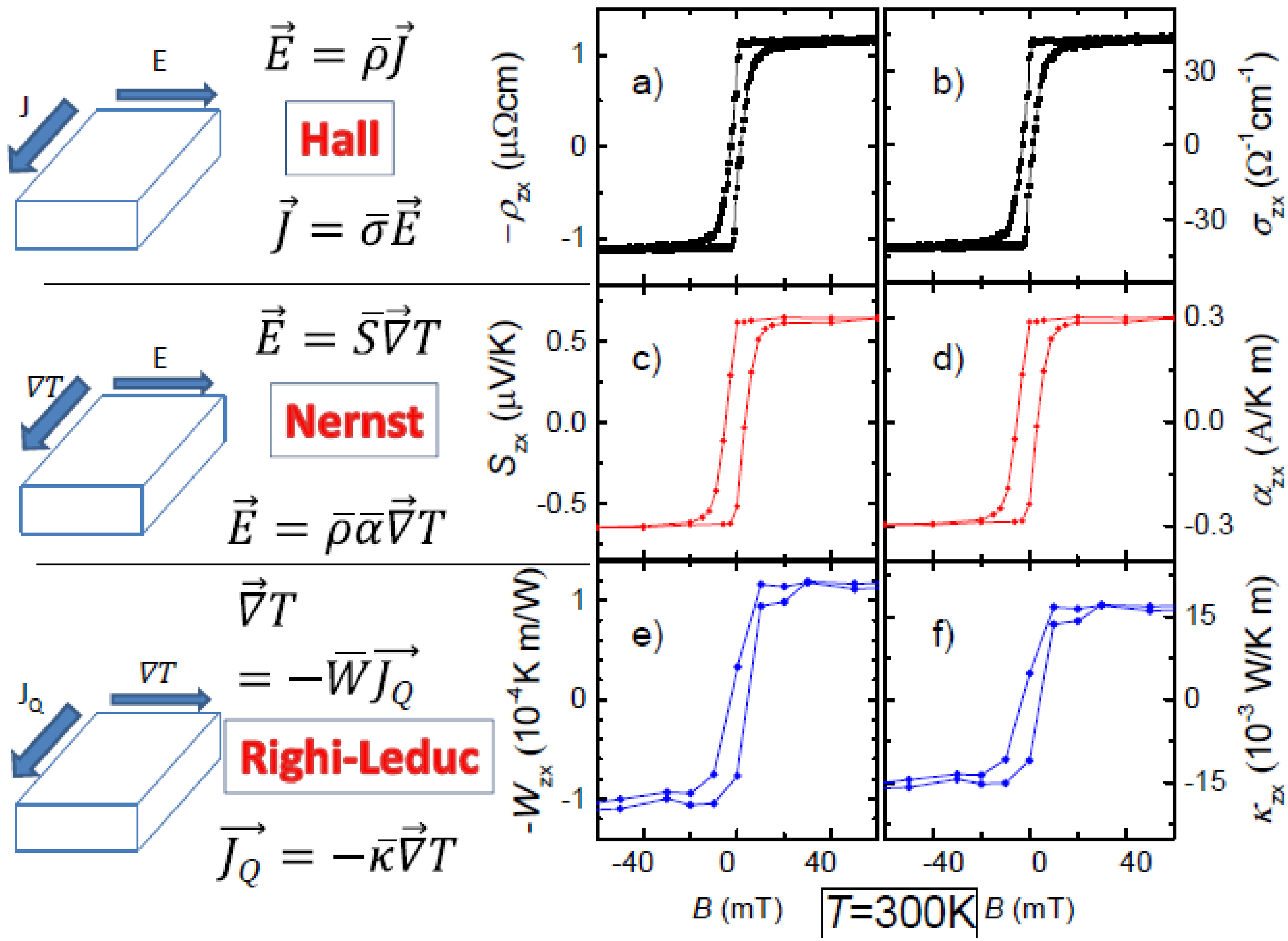

Also easily detectable transverse responses: anomalous Hall, Nernst and Righi-Leduc Effects in Mn_3Ge!

Dirty and Correlated

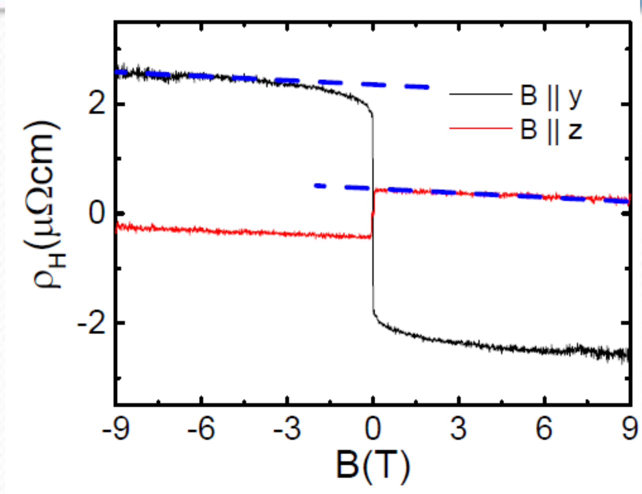

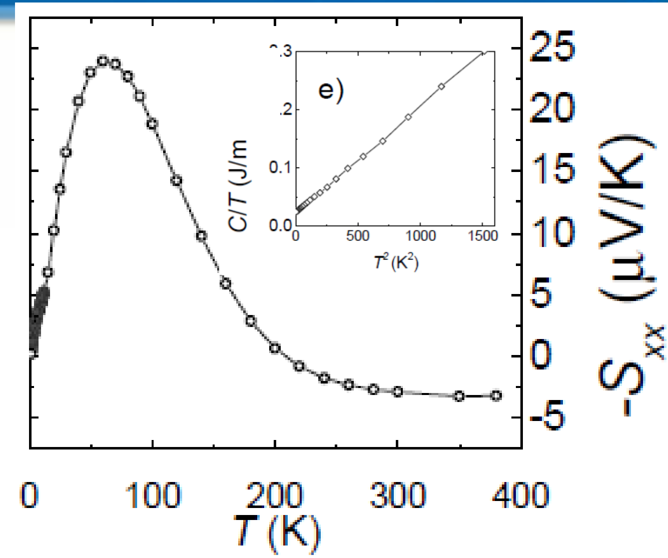

$n = 3.1 \times 10^{22} cm^{-3}$

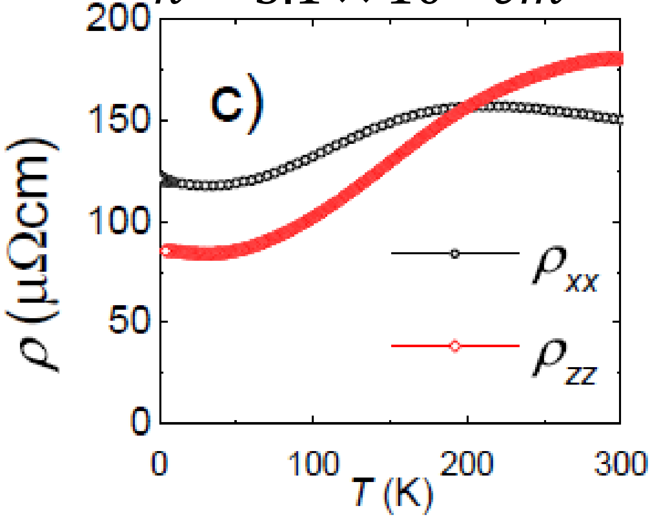

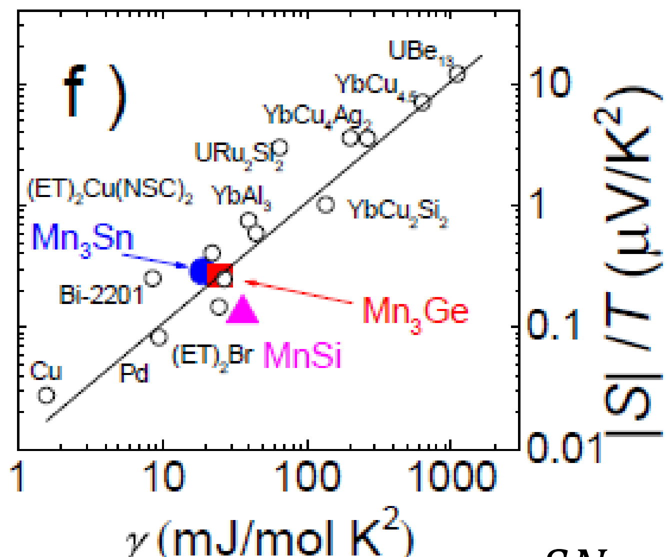

$\ell = 0.9$ nm close to the Mott-Ioffe-Regel limit

Mn:Ge: 3.32:1 to 3.35:1

10% Ge occupied by Mn l_{Ge-Ge}~1 nm

$m^* = 14.5 m_e$ $\quad q = \frac{SN_{Av}e}{T\gamma} \cong 1$

Anomalous transverse Wiedemann-Franz law

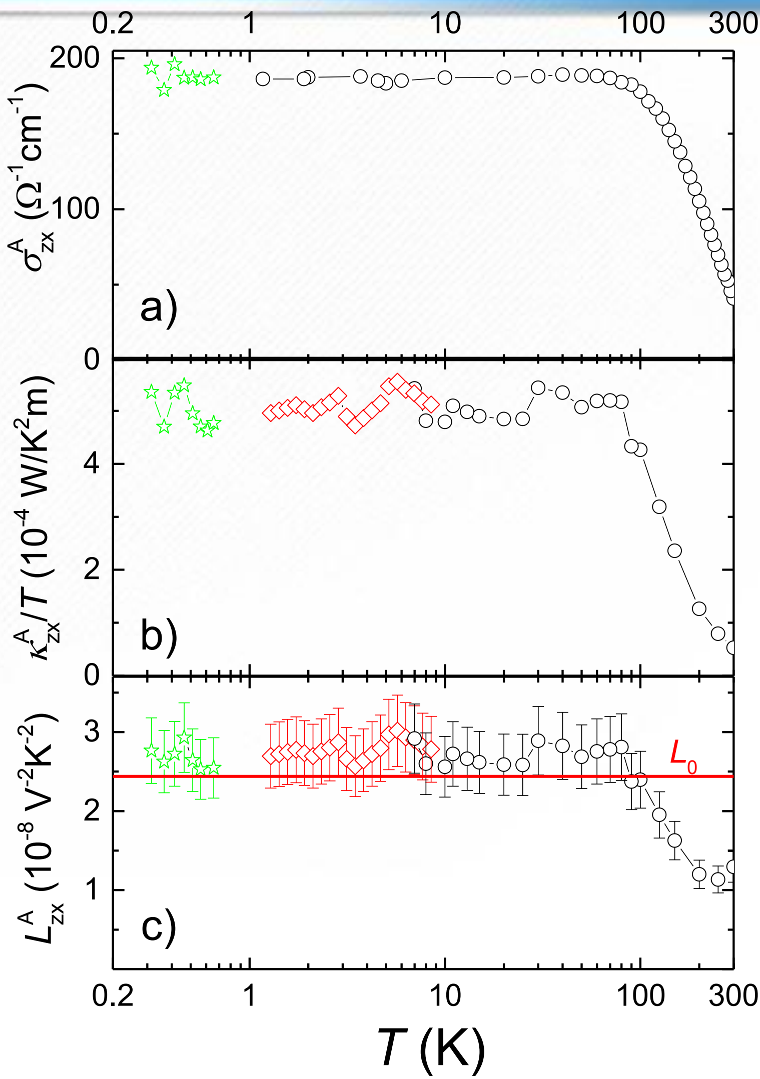

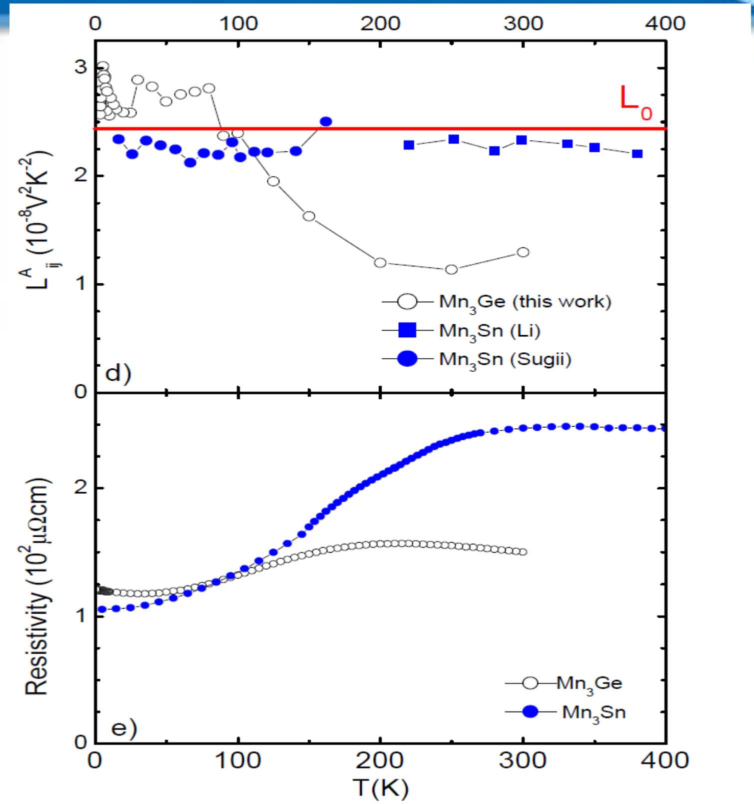

In Mn_3Sn, there is no downward finite-temperature deviation from L_0 in the whole measured range.

No inelastic scattering contribution to Anomalous Hall response.

T > 100 K, L_{zx}^A deviates from L_0, is concomitant with the decrease in σ.

Assurance of measurement

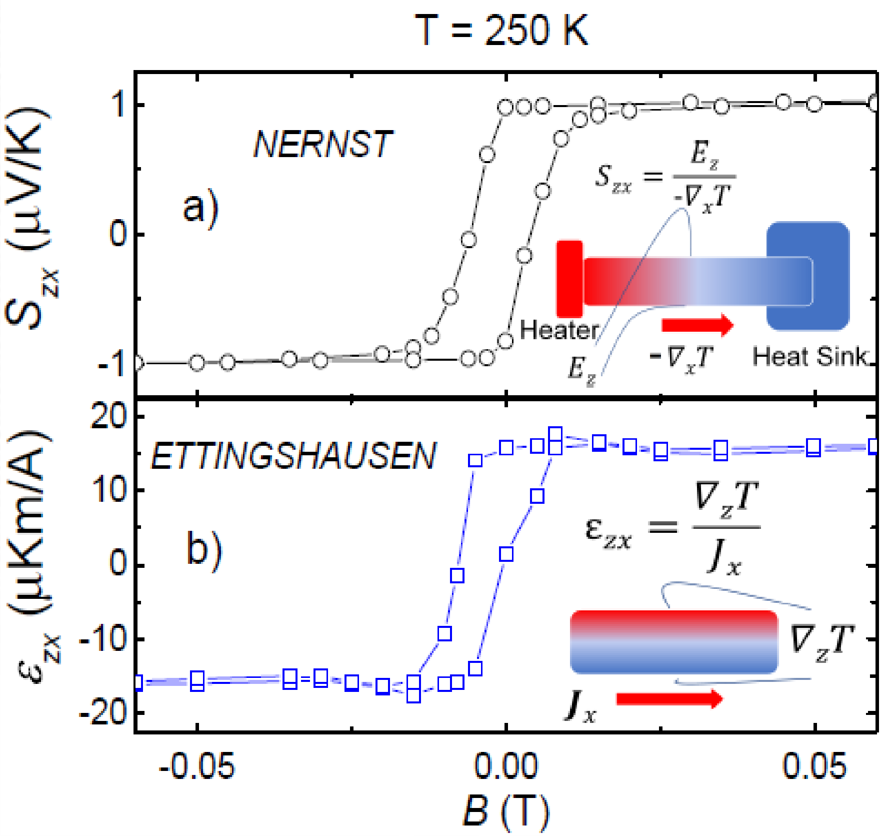

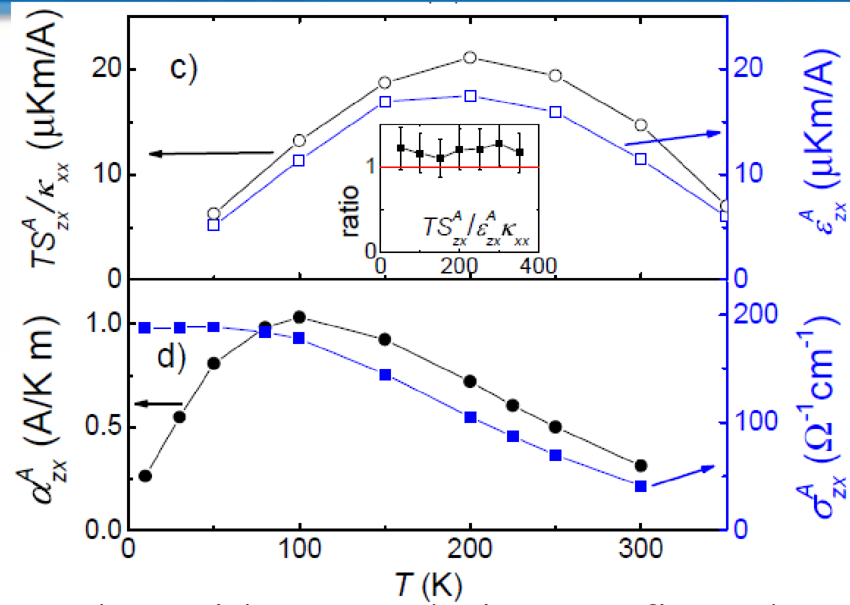

the Bridgman relation confirmed

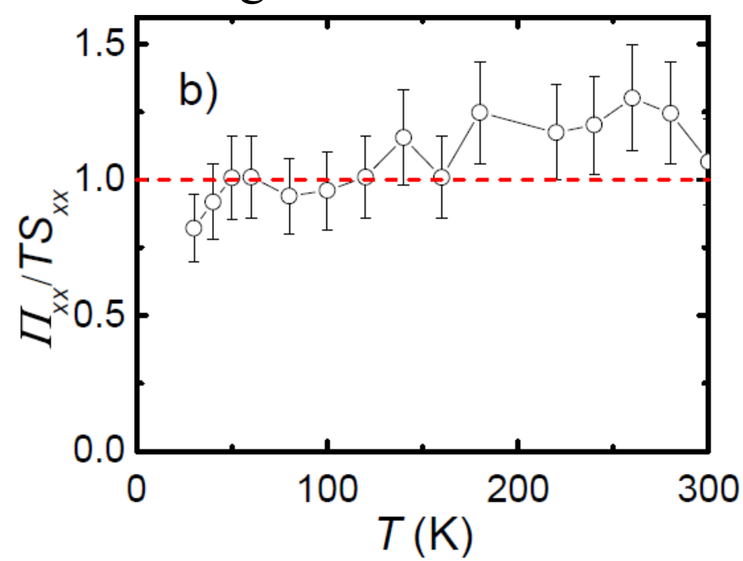

confirmed

From Onsager reciprocity:

the Bridgman relation $$\epsilon^A_{zx} = \frac{TS^A_{zx}}{\kappa_{xx}}$$

the Kelvin relation $$\Pi_{xx} = TS_{xx}$$

Violation of the anomalous transverse WF law in absence of inelastic scattering

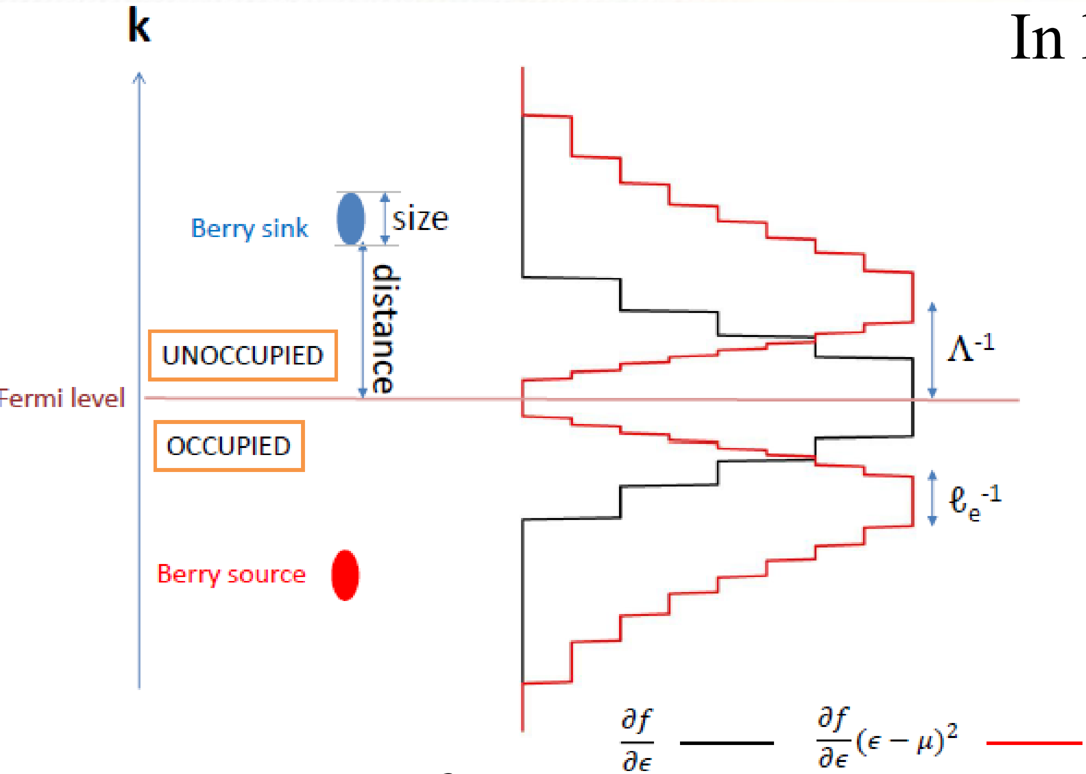

$$\sigma = -2\frac{e^2}{h}\int \frac{\partial f}{\partial \varepsilon_k}\Xi(\varepsilon)d\varepsilon$$

$$\kappa = 2\frac{ek_B^2}{h}\int [\frac{(\varepsilon-\mu)}{k_BT}]^2\frac{\partial f}{\partial \varepsilon_k}\Xi(\varepsilon)d\varepsilon$$

Transport distribution function

$$\Xi(\varepsilon) = \frac{h}{2}\int \tau(k)\, v(k)\cdot v(k)\delta\big(\varepsilon-\varepsilon(k)\big)d^{3k}$$

In k-space

1. The main source of each transport coefficient is in different location.
2. Summation extends over an interval inversely proportional to the thermal de Broglie length of electrons $\Lambda = \frac{h}{\sqrt{2\pi m^* k_B T}}$
3. l_e^{-1}, sets a minimum distance over which a Bloch wave is well-defined.

At 100 K ~ 10 meV

$$\Lambda = (\frac{h}{\sqrt{2\pi m^* k_B T}})^{-1} \sim 1\text{nm}$$

$\ell_e \sim 0.9$nm

A mismatch between thermal and electrical summations of the Berry curvature emerges!

Contrasting Mn_3Ge and Mn_3Sn in the band structure and Berry curvature

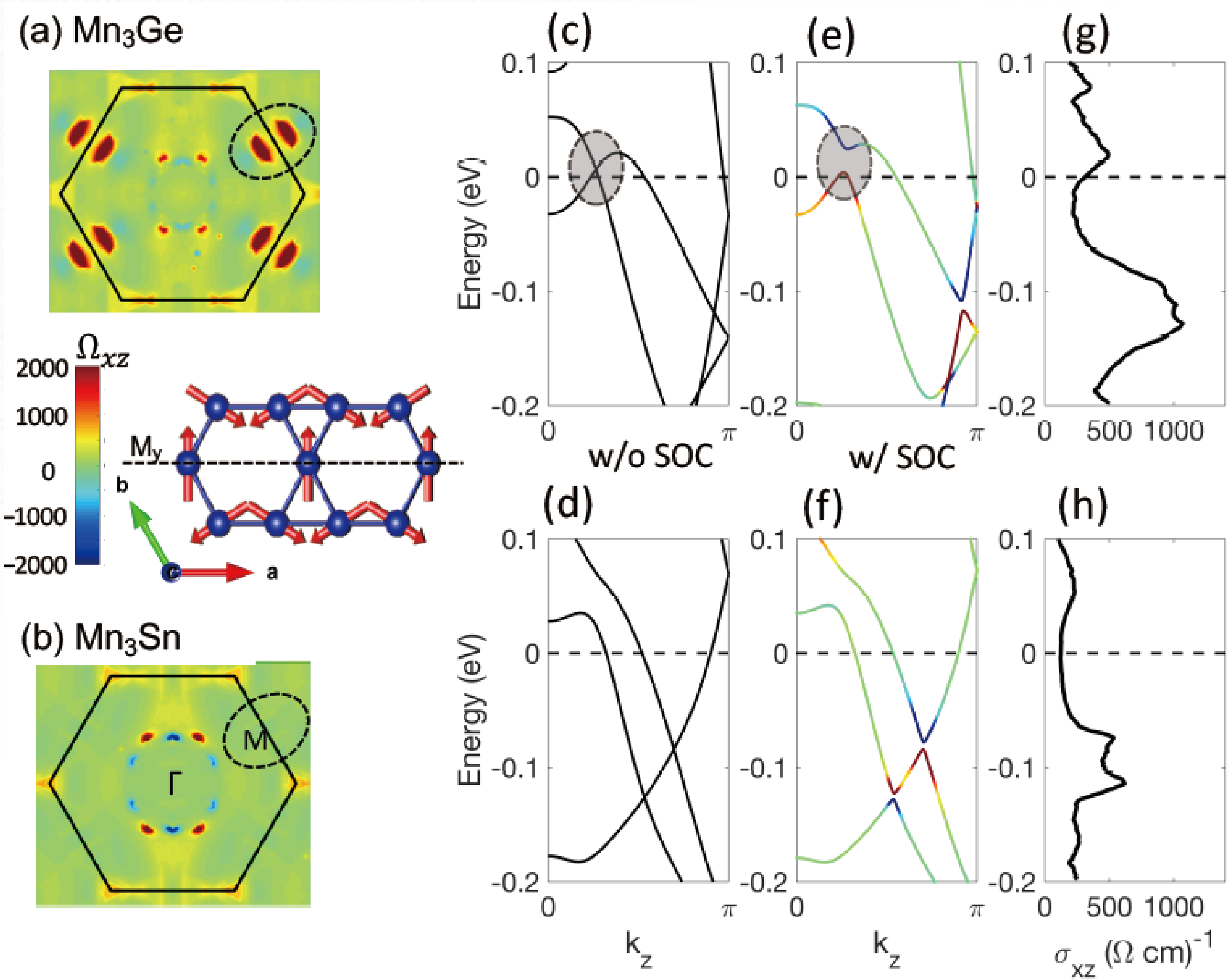

The presence of a small gap 10 meV in Mn_3Ge and its absence in Mn_3Sn is consistent with theoretical calculation.

Suggesting the hot spots at the M are the source of the Berry curvature

Liangcai Xu, et al., Z.Z* and K. B.* arXiv:1812.04339

Anomalous Hall and Nernst Effects in Mn_3Sn

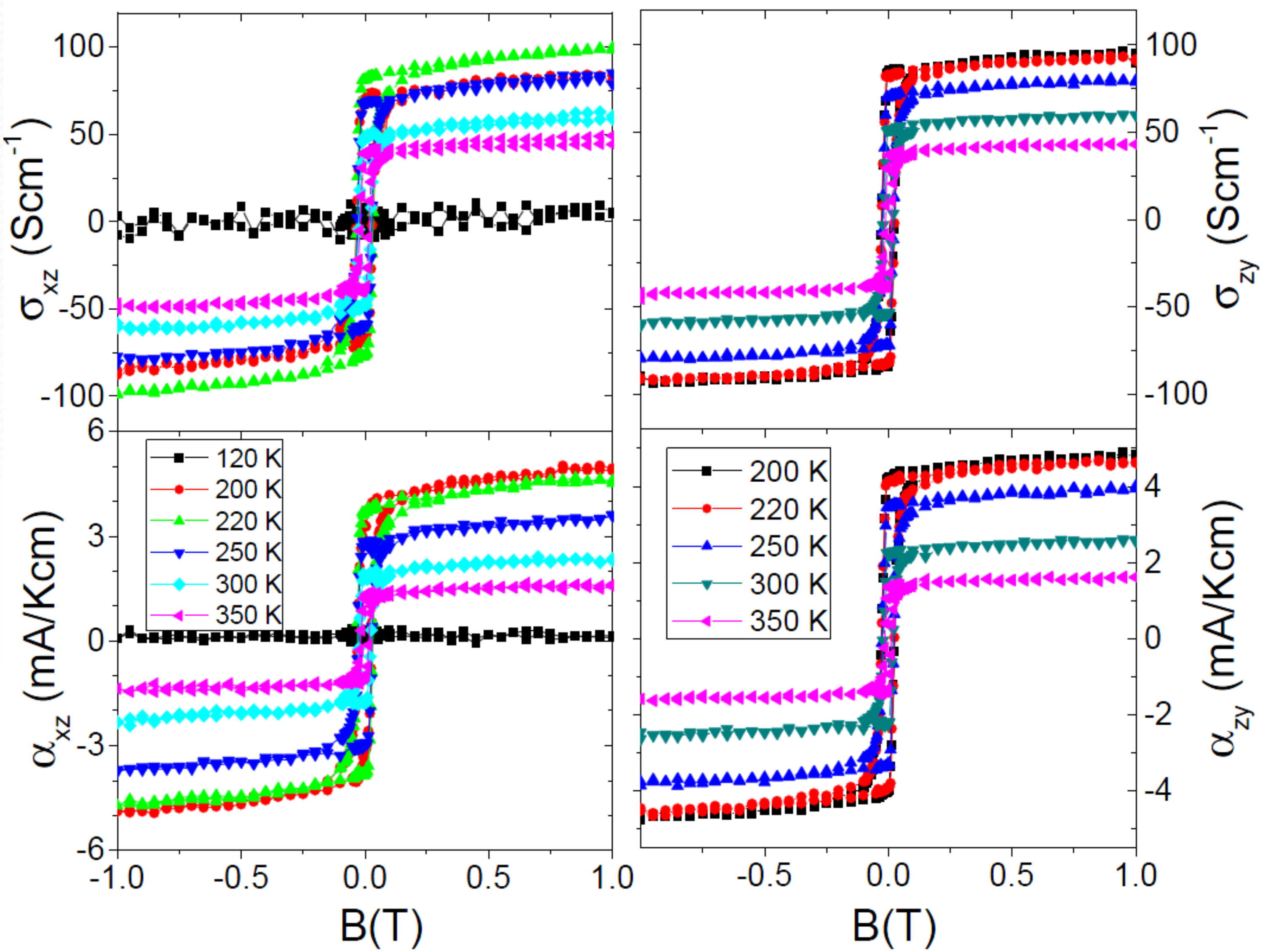

Large Temperature dependence of Anomalous Nernst Effect

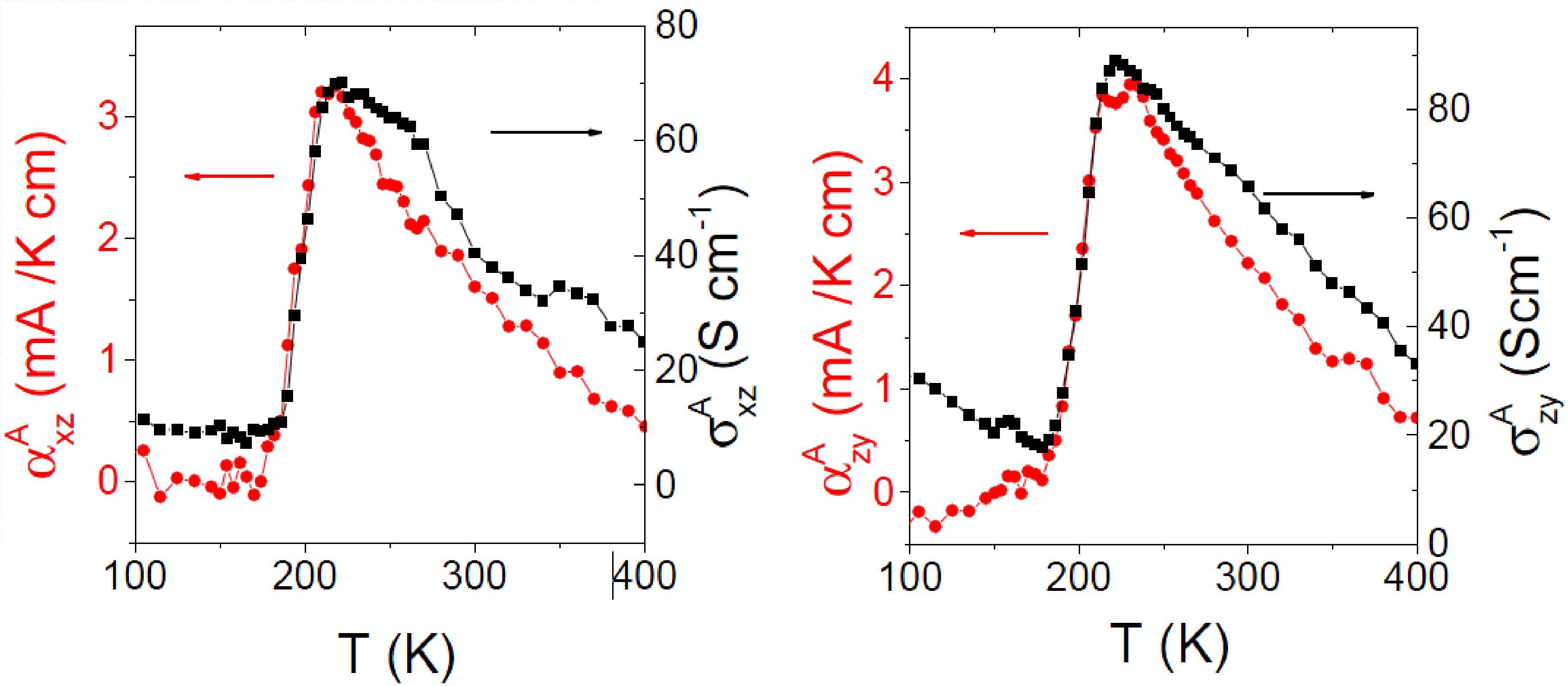

σ_{xz} changes by a factor of 3, α_{xz} by a factor of 7

Anomalous Hall and Nernst Effects in Mn_3Ge

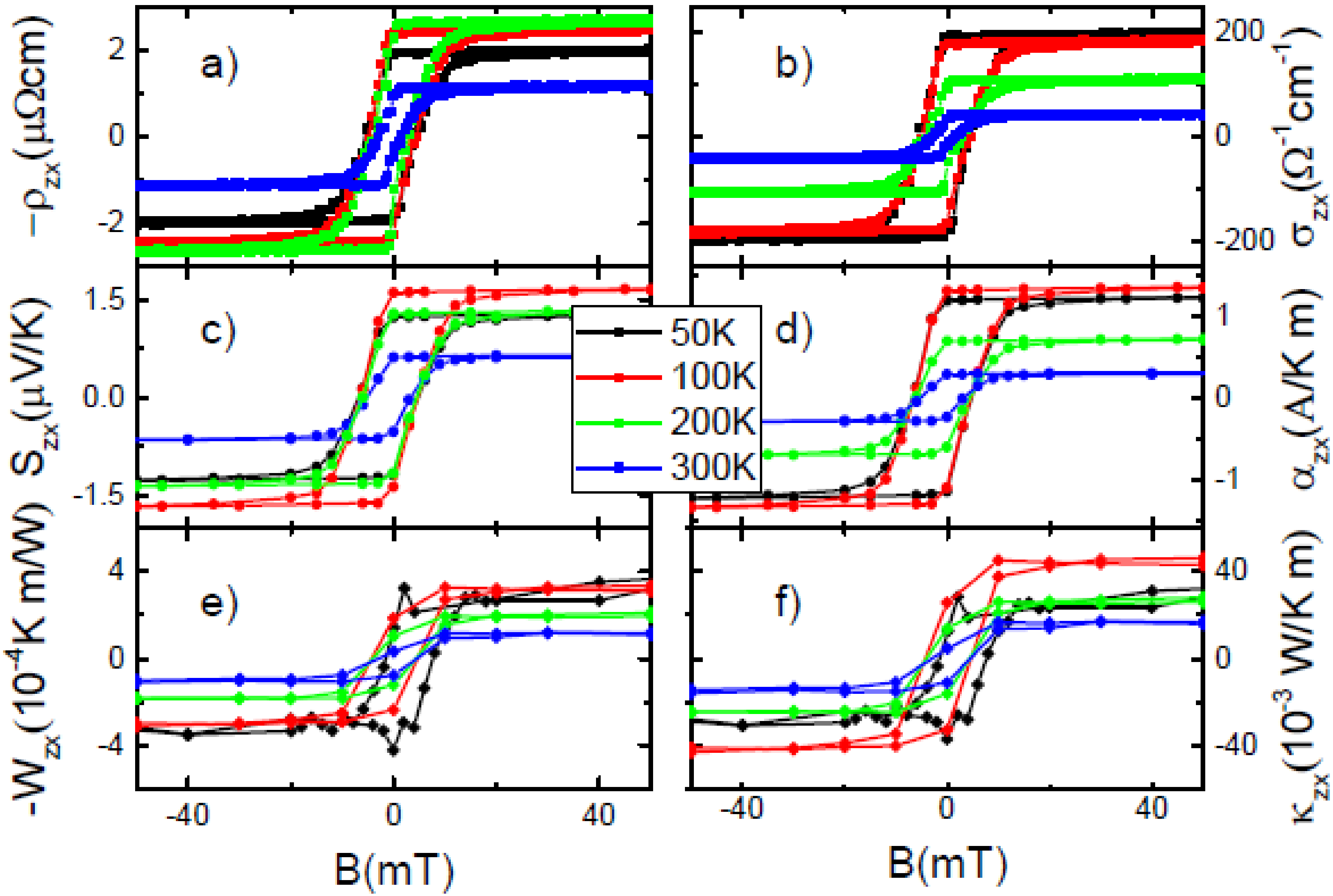

Magnitude of the AHE and ANE

The anomalous off-diagonal thermo-electric and Hall conductivities are strongly temperature dependent and their ratio is close to k_B/e.

Compounds	T	σ^A_{zy} (S/cm)	σ^A_{xz} (S/cm)	α^A_{zy} (mA/Kcm)	α^A_{xz} (mA/Kcm)	$\frac{\alpha^A_{zy}}{\sigma^A_{zy}}$ $(\mu V/K)$	$\frac{\alpha^A_{xz}}{\sigma^A_{xz}}$ $(\mu V/K)$
Mn_3Sn	400 K	32	25	0.7	0.5	21.9	20
	200 K(Max)	90	72	3.9	3.2	43	44
Mn_3Ge	300 K		40.8		0.31		76

Ordinary and topological Hall effects

Ordinary

$$\sigma_{xy} = -\frac{e^2}{\hbar}\int_{BZ}\frac{d^3k}{(2\pi)^3}\ell^2$$

Depends on the mean-free-path!

Topological

$$\sigma_{xy} = -\frac{e^2}{\hbar}\int_{BZ}\frac{d^3k}{(2\pi)^3}\Omega^Z(k)$$

Does not depend on the mean-free-path!

$$\boxed{\frac{\alpha_{xy}}{\sigma_{xy}} = \frac{k_B}{e}F(<|\Omega^Z>)}$$

=86 μV/K

$$S = \frac{\alpha}{\sigma} = \frac{k_B}{e}\frac{<k_{dB}^2>}{<k_F^2>} = \frac{\pi^2}{3}\frac{k_B}{e}\frac{T}{T_F}$$

The specialties of domain wall:

Momentum-space and real-space Berry curvatures in Mn_3Sn

---Xiaokang Li, et al., Z.Z*, K.B* Scipost Phys. 5, 063 (2018)

Chiral domain walls of Mn_3Sn and their memory

---Xiaokang Li, et al. , Z.Z*, K.B* arXiv:1903.03774 (2019)

Shape of hysteresis

Sigmoid shape in ferromagnets:

Fe-C 0.06wt%

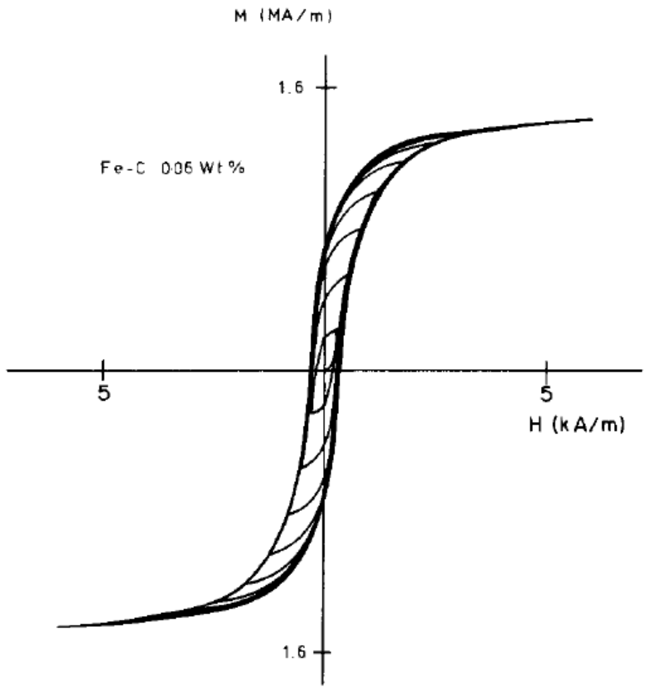

Fig. 11. Experimental magnetic hysteresis loops for a spec of Fe–C 0.06 wt%.

K. Everschor-Sitte and M. Sitte, J. Appl. Phys. 115, 172602 (2014).

Symmetric hysteresis in QAHE:

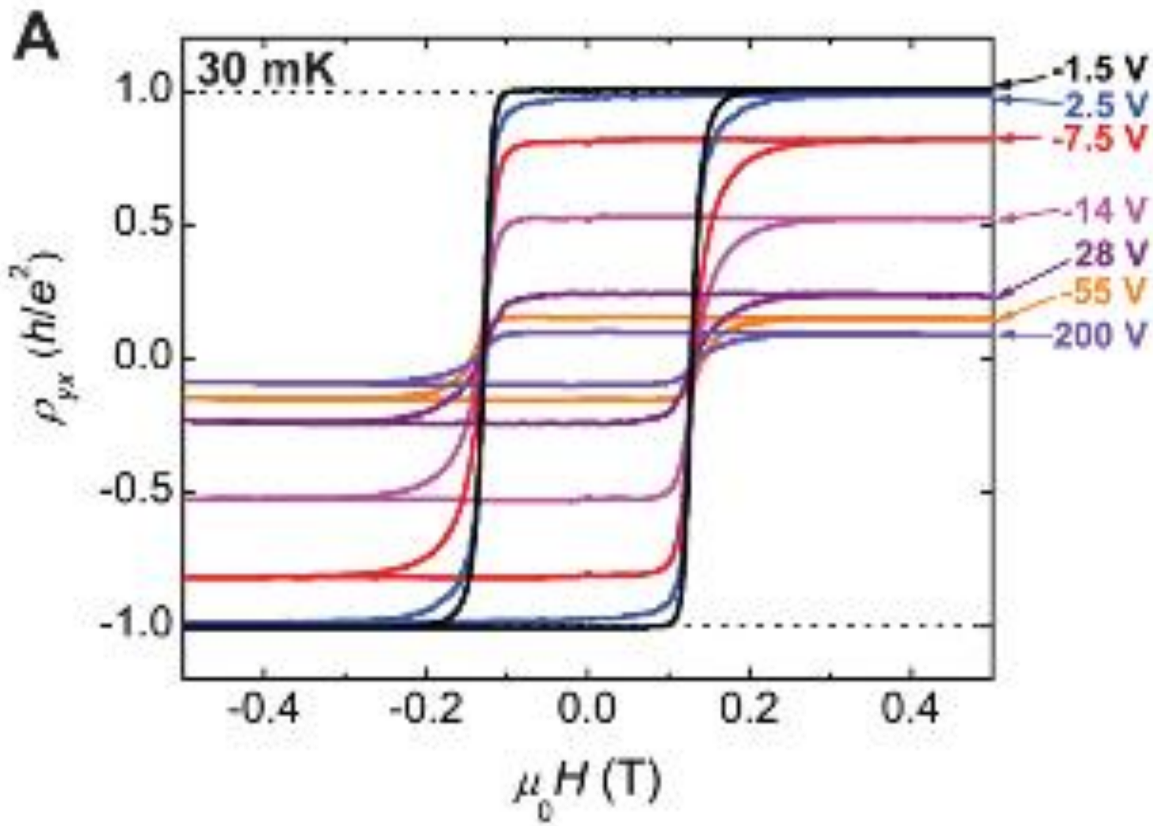

C. Z. Chang et al., Science 340, 167 (2013)

Peculiar hysteresis in Mn_3Sn

Independent of sweeping rate!

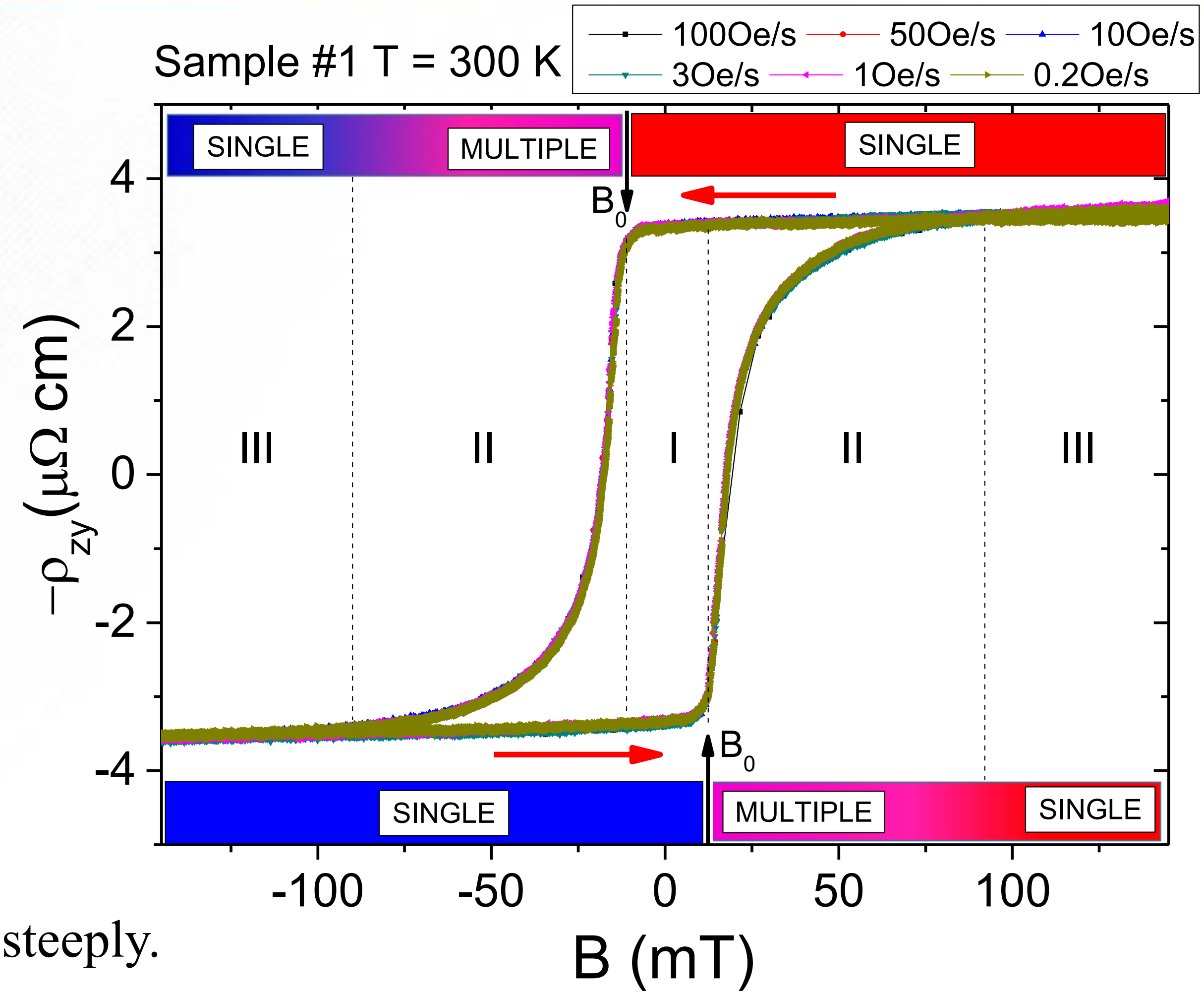

At B_0: $\rho_{ij}(B)$ begins to change steeply.

Regime I: single-domain

Regime II: multi-domain

Regime III: field-induced single domain

sharp

fuzzy

To illustrate the difference between three regimes

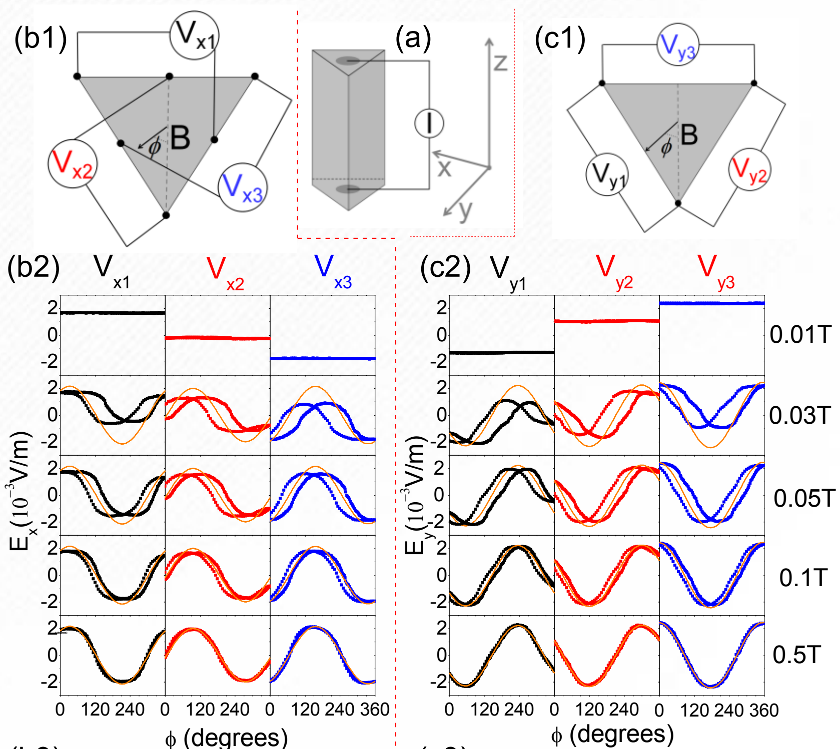

Measurement configuration

Regime I, unaffected

Regime II, strong hysteresis

Regime III, each E_x and E_y is perfect sinusoidals.

Indicating:

1). Single-ion anisotropy is very weak. $0.5\mu eV/f$.u. ($1.5 \times 10^{-2}\mu_B/f$.u. at 0.5 T)

~ 0.2 μeV per Mn APL 107, 082404 (2015)

2).isotropic in-plane momentum-space Berry curvature.

Isotropic in-plane momentum-space Berry curvature

Anomalous Hall effect:

$$\sigma_{ij}^{A} = \frac{-e^2}{\hbar}\sum_{n}\int_{BZ}\frac{d^3k}{(2\pi)^3}f_n(k)\Omega_n^k(k)$$

Implications for the Weyl nodes in k-spaces:

σ_{ij} remaining finite is not set by a crystal axis.

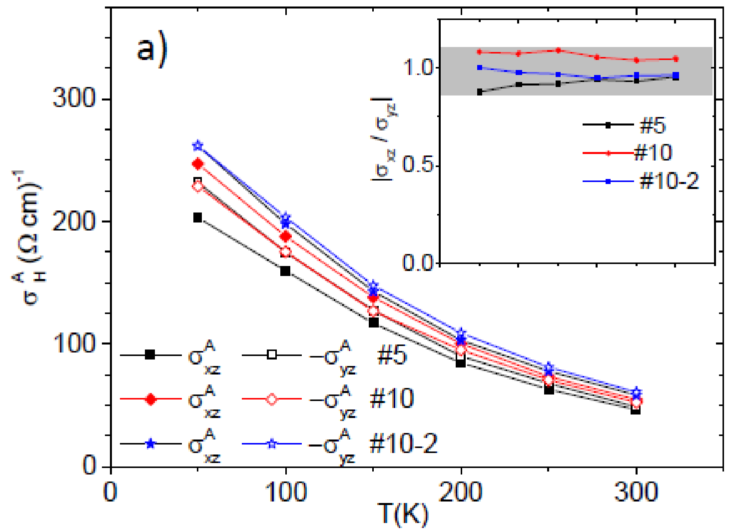

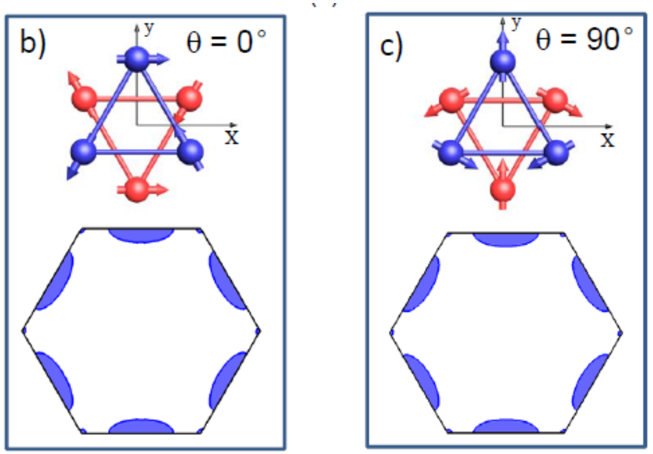

In-plane anisotropy: ~0.05

agrees with our DFT calculation

Domain nucleation at the onset of regime II

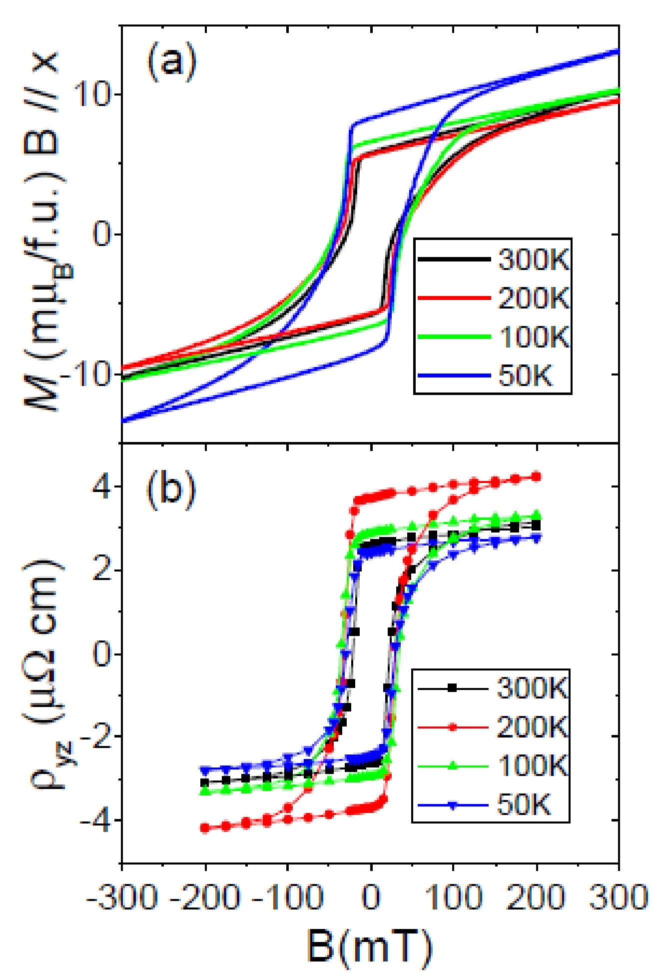

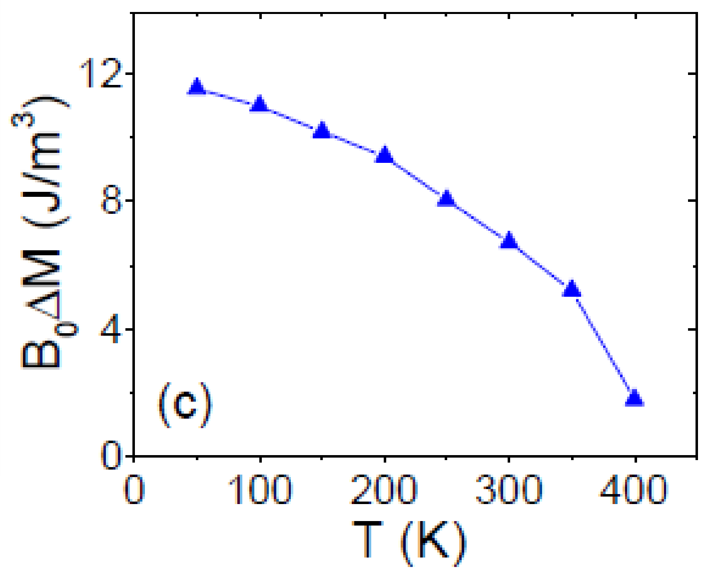

B_0 is identical in both M and Hall resistivity

The volume energy: $E_v = B_0 \Delta M$

According to the classical theory of nucleation:

the domain-wall energy $E_s = \langle J \rangle / t^2$

$$t = \left(\frac{< J >}{B_0 \Delta M}\right)^{1/3} \qquad <J>\sim 5meV \qquad t \geq 100\ nm$$

consistent with PRL 119, 176809 (2017)

Real-space Berry curvature (skyrmion)

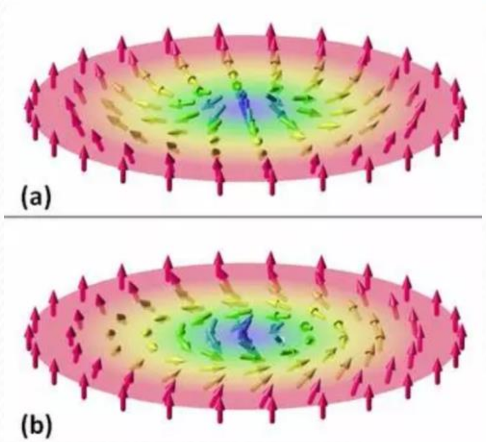

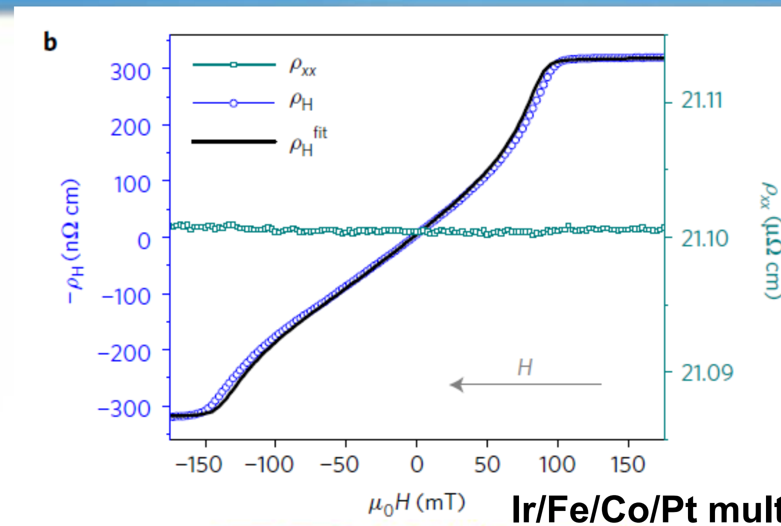

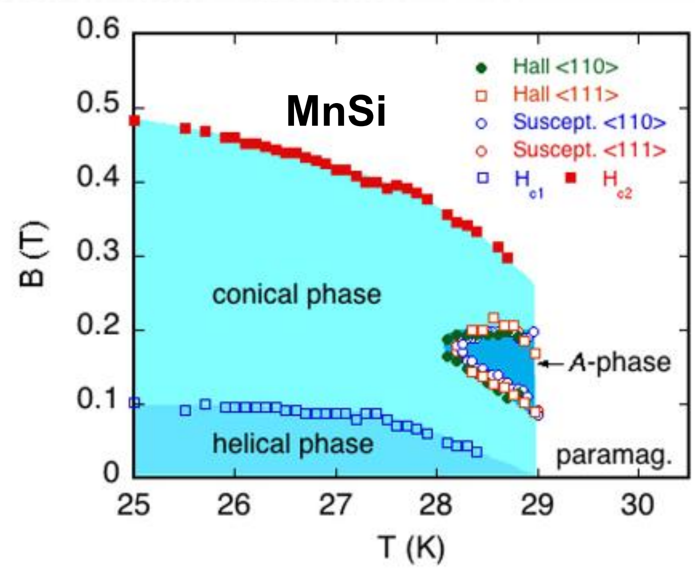

Ir/Fe/Co/Pt multilayers

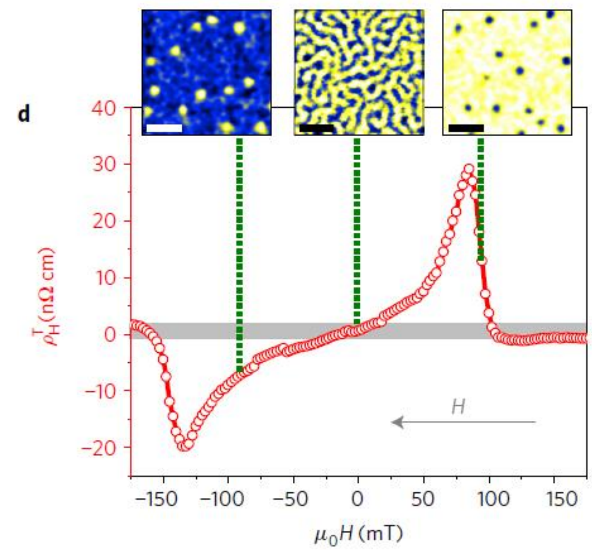

A. Neubauer, et al., Phys. Rev. Lett. 102, 186602 (2009).

A.Soumyanarayanannnkd et al., Nat. Mater.16, 898(2017)

Topological Hall effect(THE) caused by real-space Berry curvature

Berry curvature in real space: Topological Hall effect

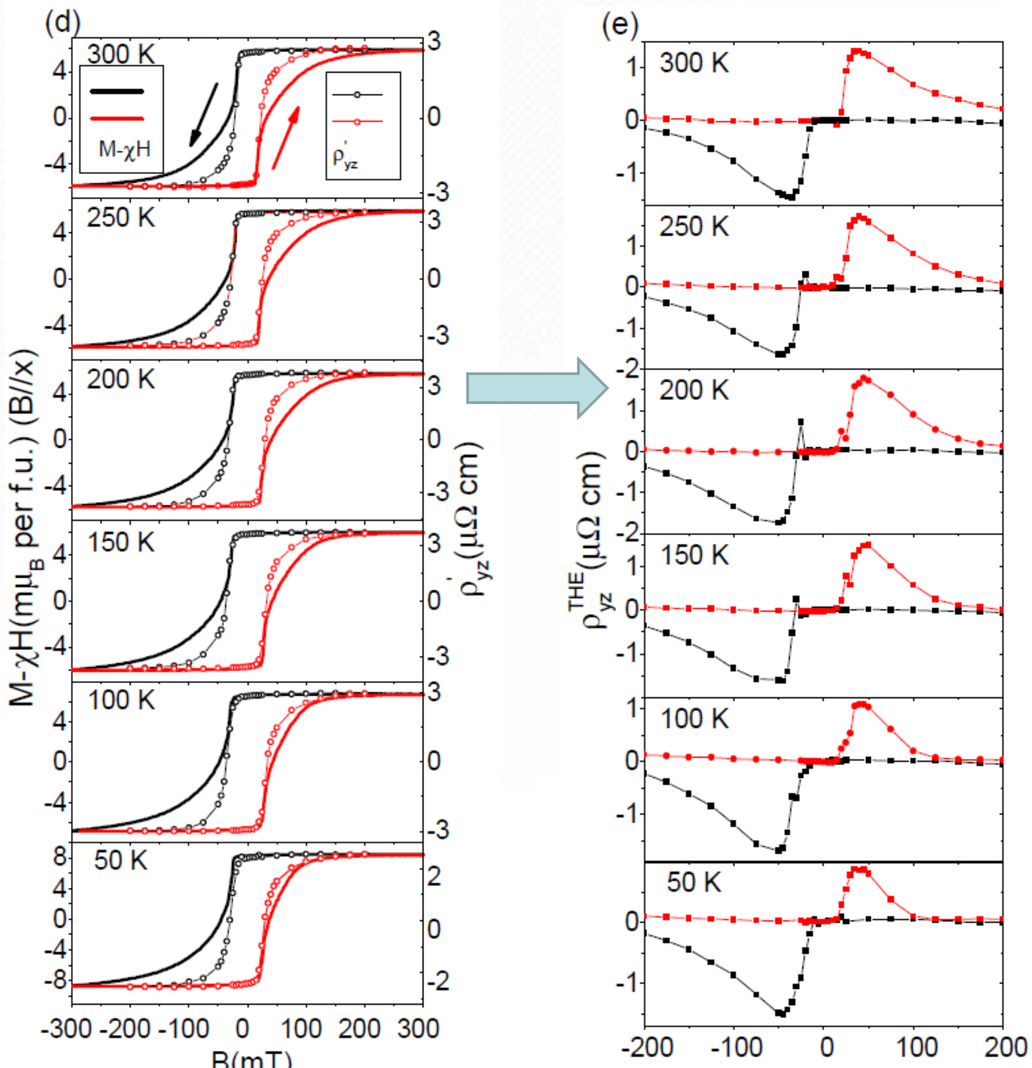

After subtracted normal part

THE

	σ_H^A	σ_H^{THE}	M	S_H	$\frac{\sigma_H^{THE}}{\sigma_H^A}$
	S/cm	S/cm	A/cm	V^{-1}	
MnSi	56[7]	1.8[7]	293.8 [8]	0.19	0.032
Mn_3Sn	232	113.7	10.75	21.6	0.49

$$S_H = \sigma_H^A / M$$

Comparison of magnetization and AHE in Mn_3Sn (at 50K) with MnSi (at 28 K).

How the THE comes?

A finite THE is expected as $\vec{n}\cdot\left(\frac{\partial\vec{n}}{\partial x}\times\frac{\partial\vec{n}}{\partial y}\right)$ is finite. $\vec{n}=\vec{M}/\mathrm{M}$: the skyrmion density.

1). A non-coplanar component needed

2). A particular spin configuration without inversion center between two domains of opposite chirality.

Skyrmions are expected to arise in the presence of the Dzyaloshinskii-Moriya interaction and the absence of the inversion center.

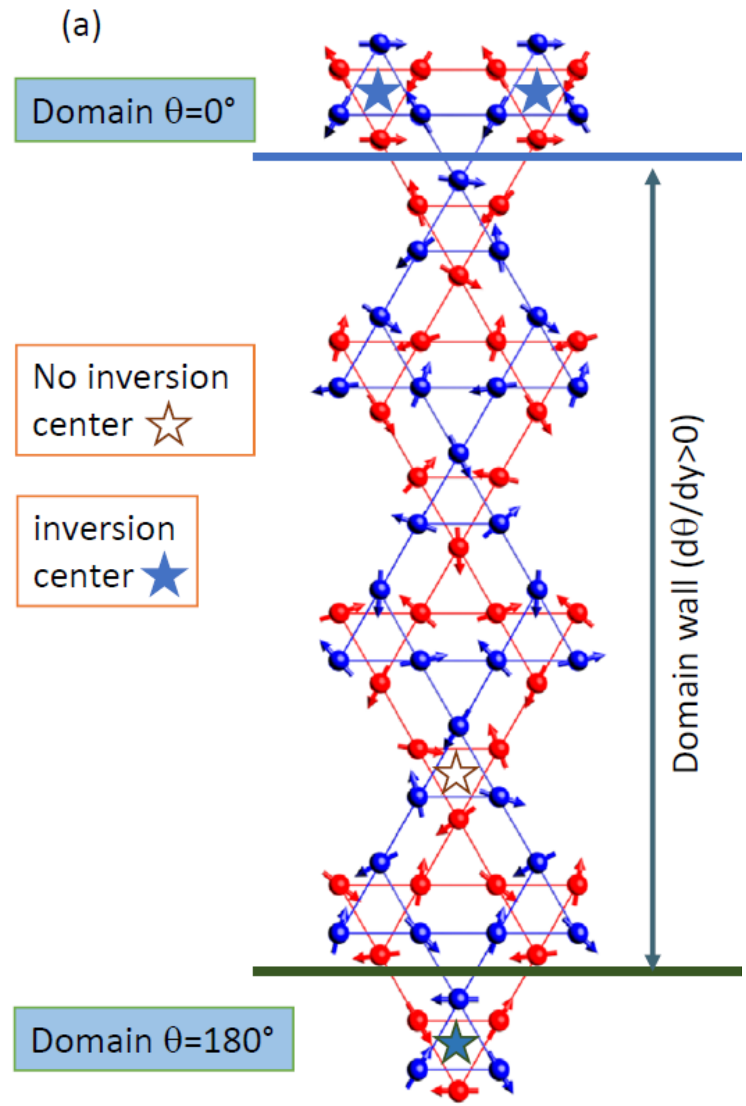

Size dependence of B_0 and B_s (nontrivial domain walls)

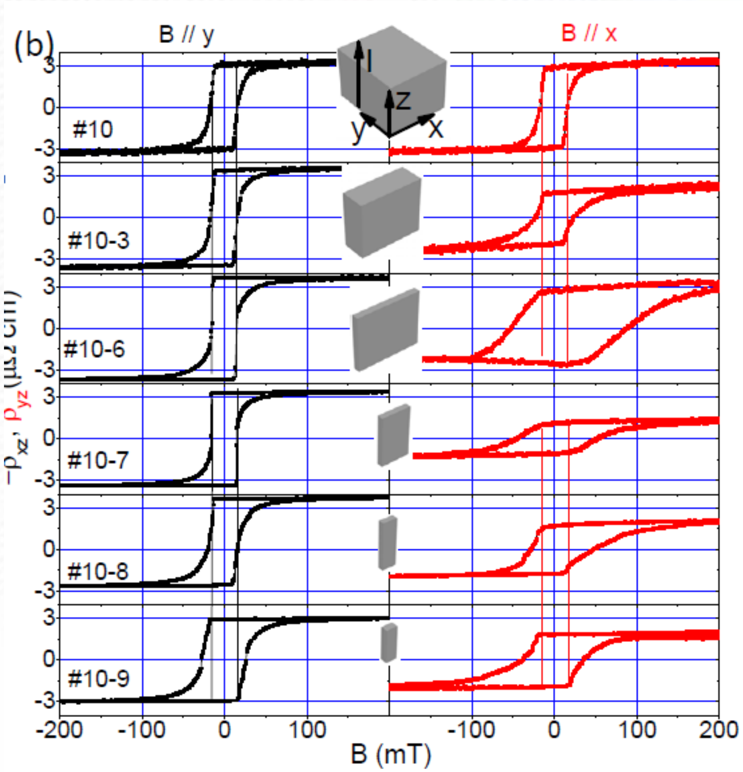

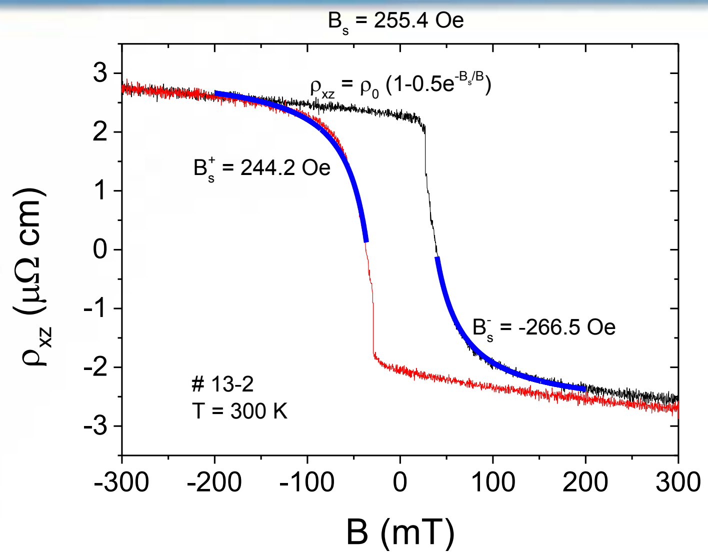

B_s is a measure of hysteresis width

1. Reducing size does not affect B_0 and AHE

2. B_s anisotropy is equal to the anisotropy of the sample dimensions.

hitherto unreported component Hall and Nernst responses

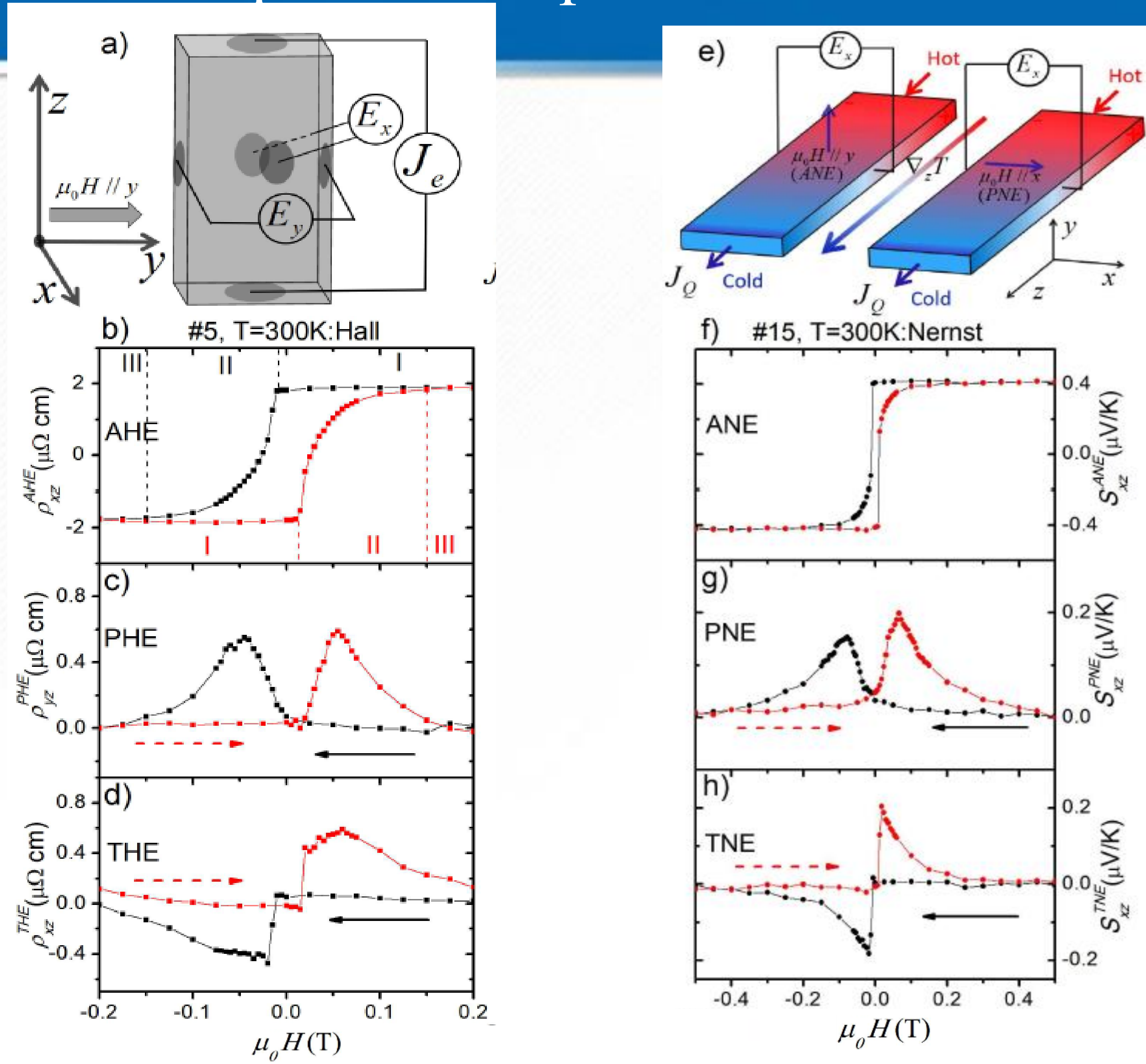

Planar Hall resistivity (ρ_{yz}^{PHE}), extracted from E_y. Topological Hall resistivity (ρ_{xz}^{THE})

Planar Nernst effect (S_{xz}^{PHE}). Topological Nernst effect (ρ_{xz}^{THE})

1. different signs
2. constant ratio

Anomalous, topological and planar Hall (Nernst) effect discovered in Mn_3Sn

hitherto unreported component Hall and Nernst responses

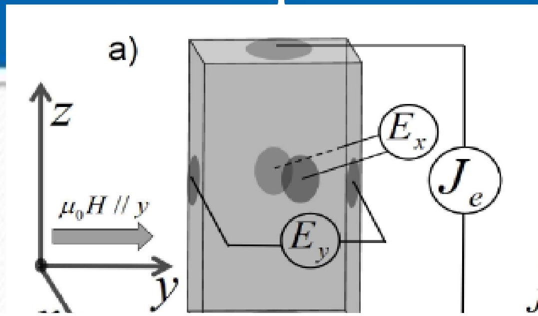

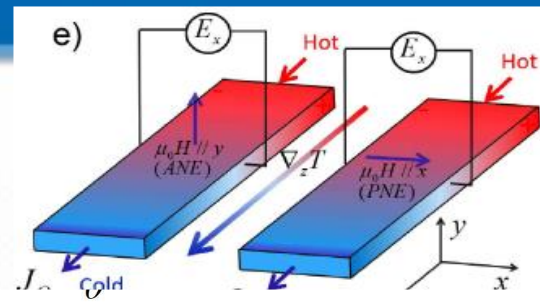

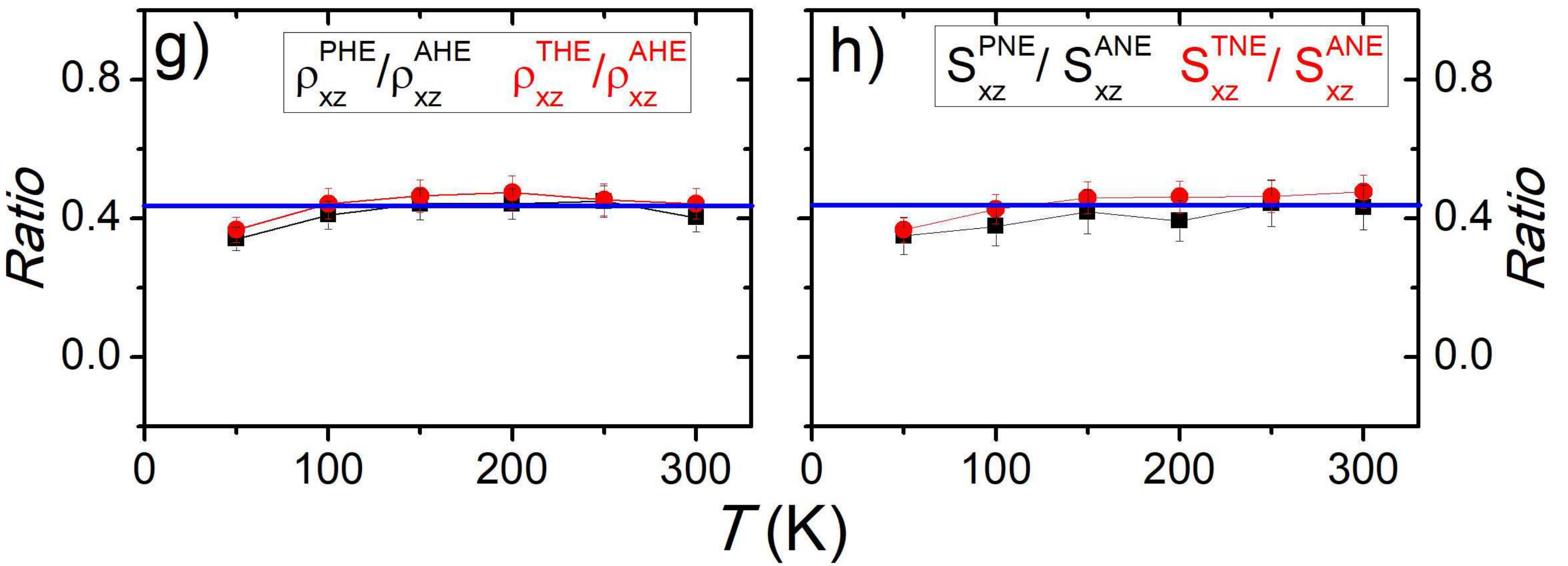

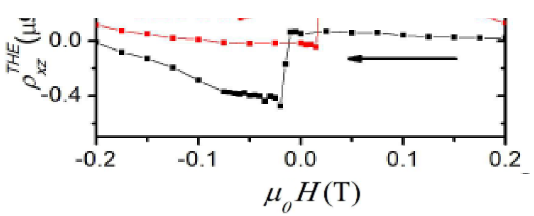

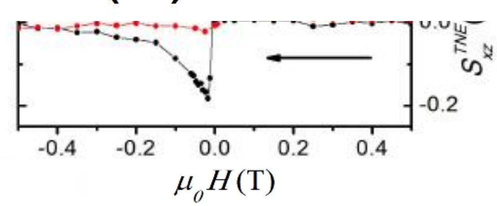

1. different signs
2. constant ratio

Anomalous, topological and planar Hall (Nernst) effect discovered in Mn_3Sn

Longitude and transverse magnetization

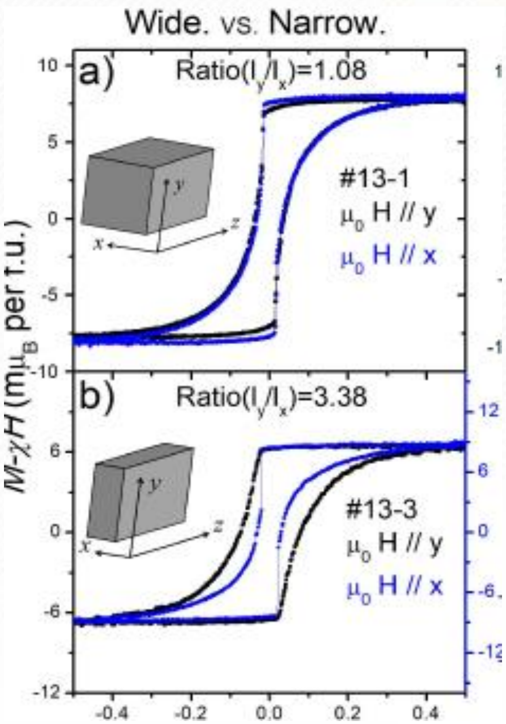

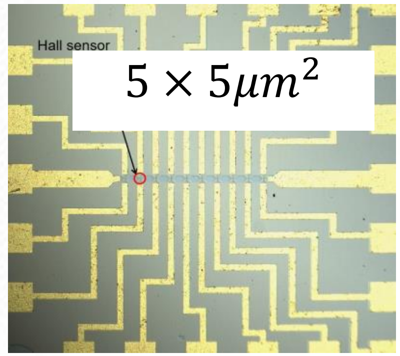

Micron-size 2DEG Hall sensors

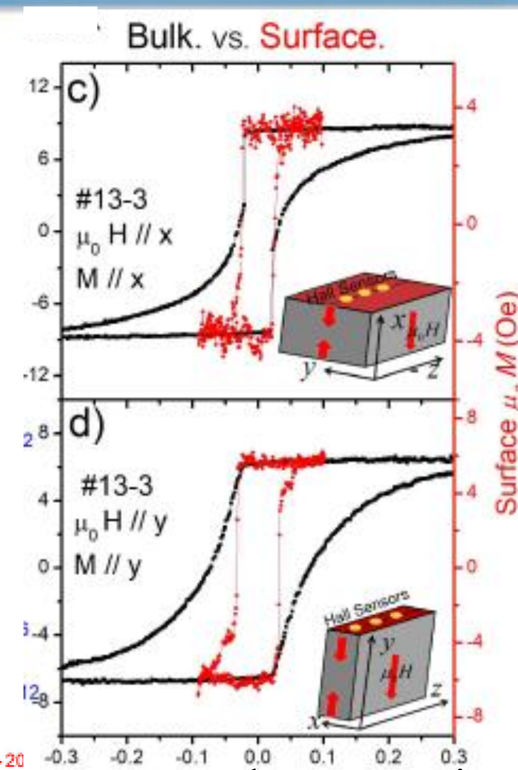

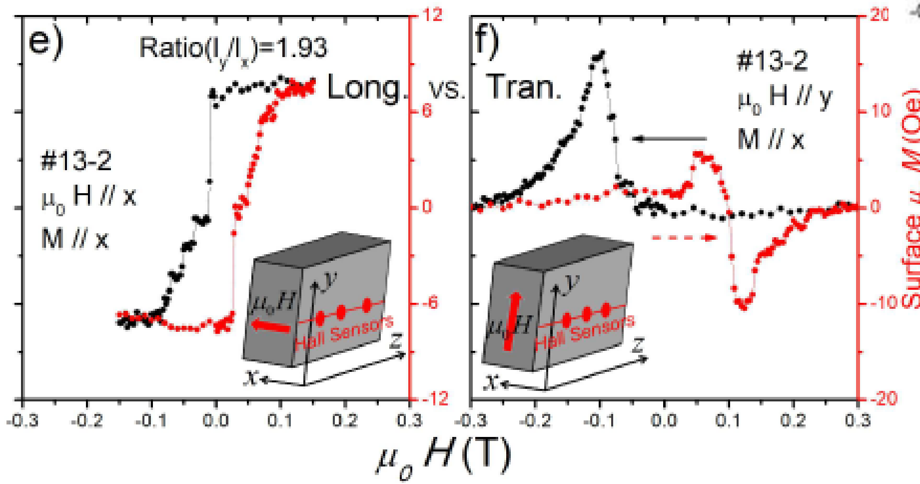

smooth occupation of the center

Having transverse response! restricted to regime II

A spin texture for domain walls:

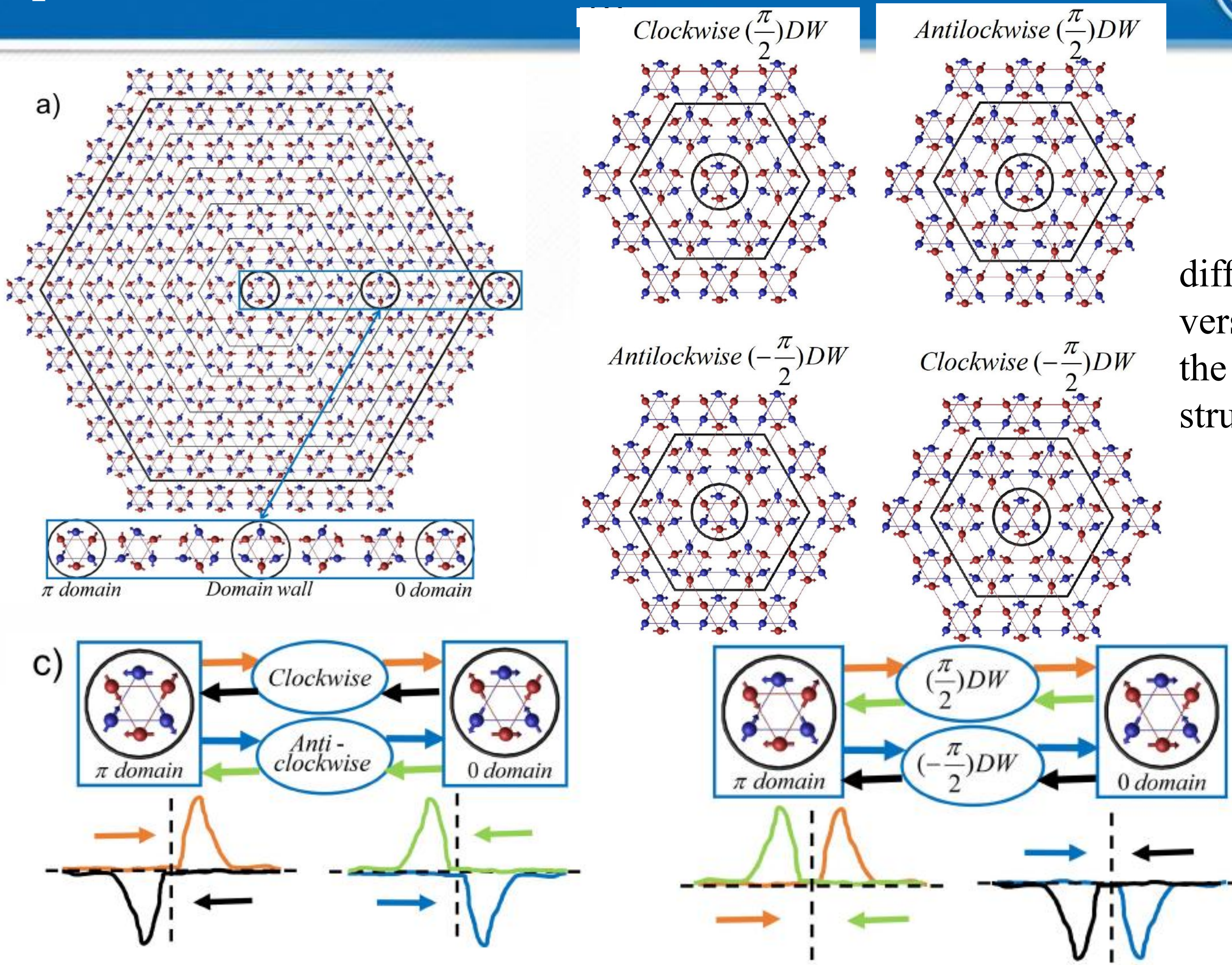

different versions of the same structure

Memory of direction

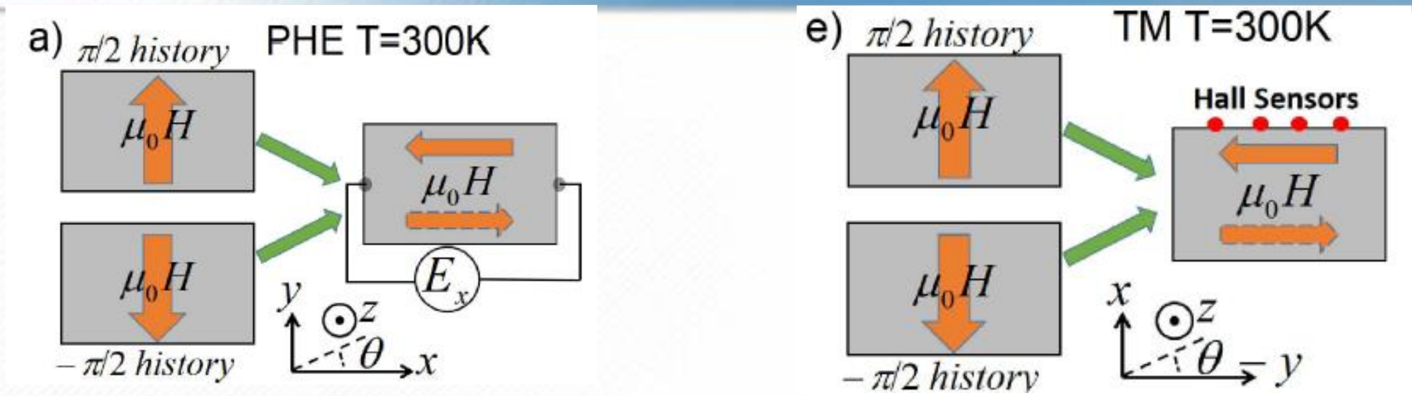

Identical configuration but with different prior histories

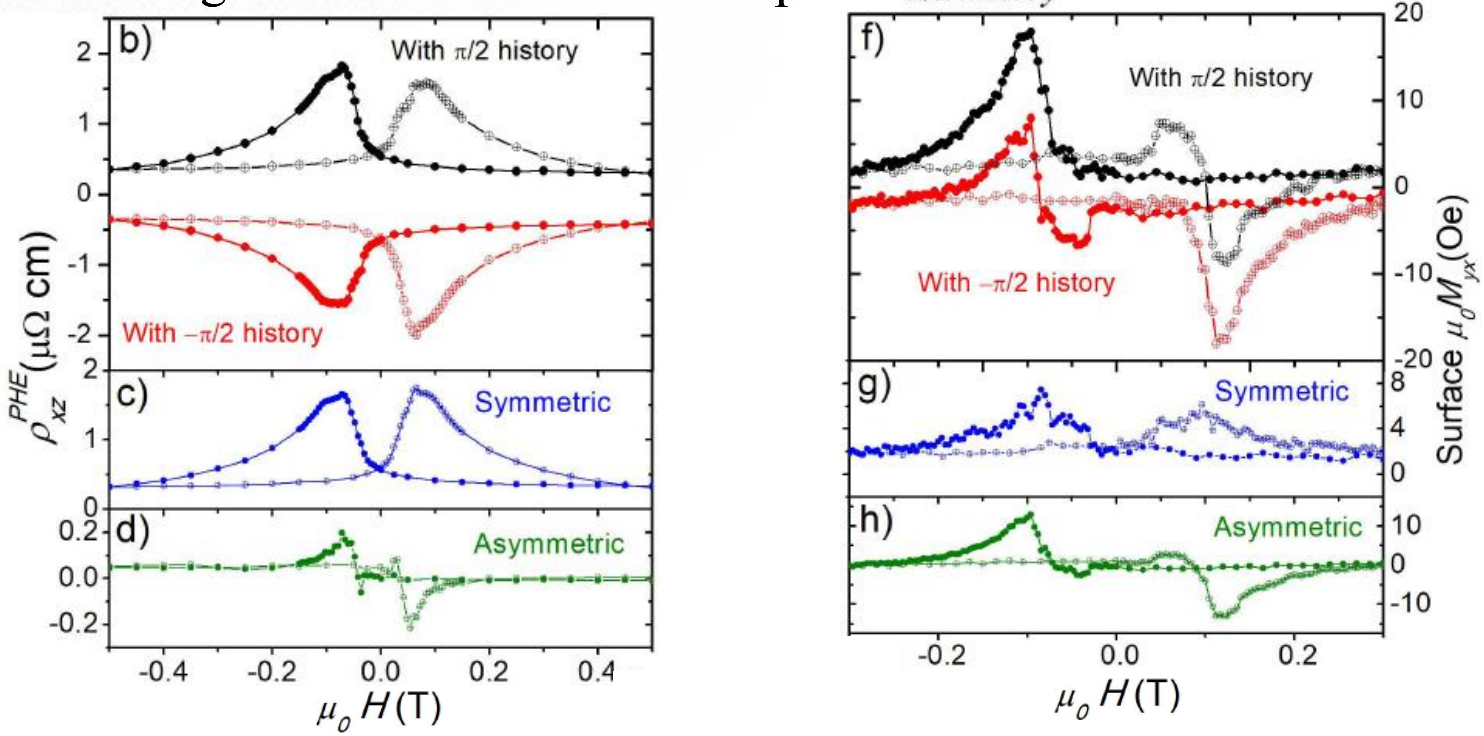

The orientation of the spins inside walls is mainly set by the past history.

Evolution of the PHE signal with amplitude of prior field:

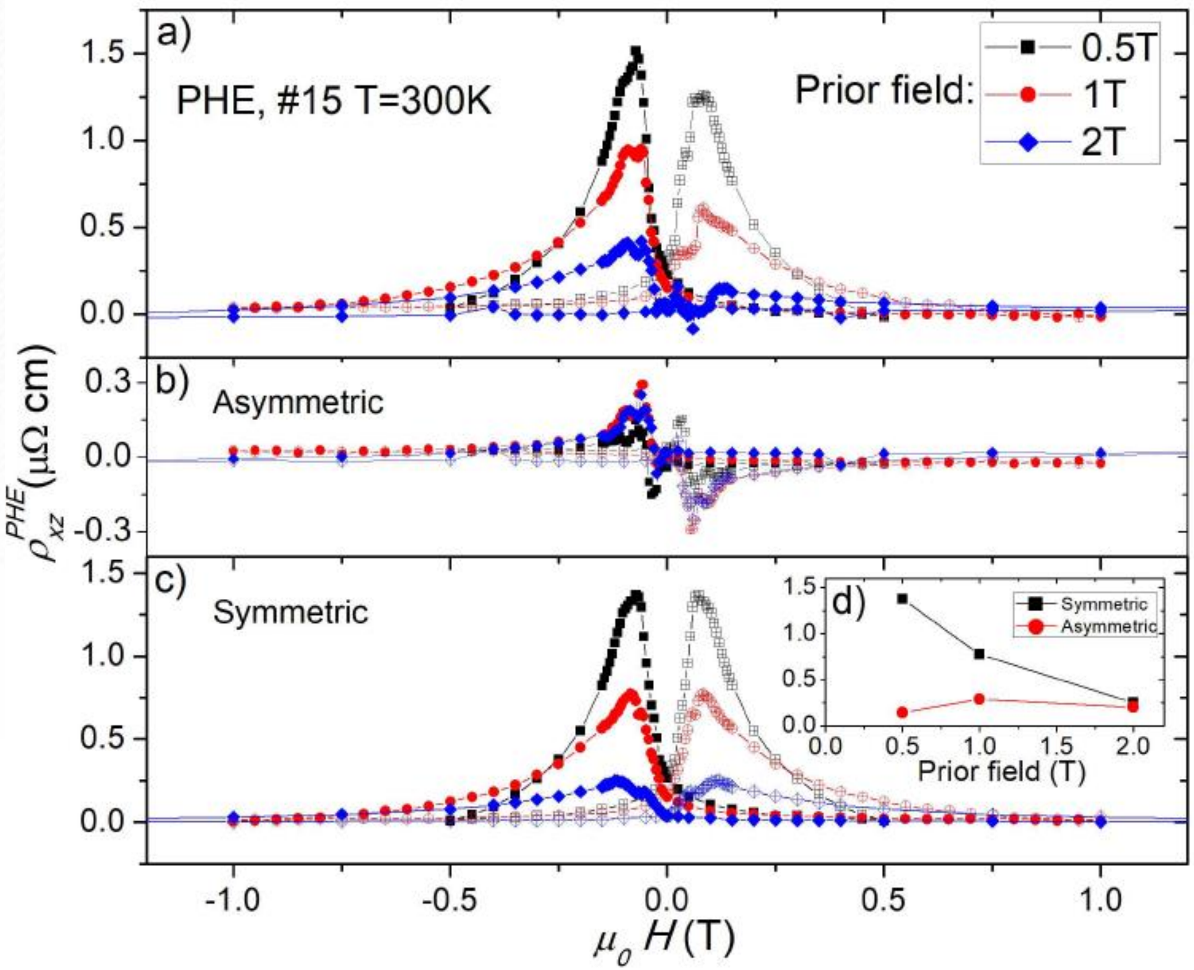

The symmetric component of the PHE set by the chirality of the wall is promoted by the presence of minority domains to stock information.

Summary

1. Validity of the WF law in transverse confirms that Anomalous Hall Effect is a Fermi surface property.
2. Violation of the anomalous transverse WF law in absence of inelastic scattering in Mn_3Ge.
3. The anomalous off-diagonal thermo-electric and Hall conductivities ratio is close to k_B/e.
4. In regime II, there are multiple magnetic domains and an additional component due to the real-space Berry curvature.
5. The Mn_3Sn has chiral domain walls, depending on the history of the field orientation and can be controlled.

Thanks for your attention!

Xiaokang Li, et al., Z.Z*, K.B* PRL 119, 056601 (2017)
Xiaokang Li, et al., Z.Z*, K.B* Scipost Phys. 5, 063 (2018)
Liangcai Xu, et al., Z.Z* and K. B.* arXiv:1812.04339
Xiaokang Li, et al., Z.Z*, K.B* arXiv:1903.03774